Differential-geometric Considerations on the Hodograph Transformation for Irrotational Conical Flow

PROEFSCHRIFT

Ter verkrijging van de graad van doctor in de technische wetenschap aan de Technische Hogeschool te Delft, op gezag van de Rector Magnificus Dr. R. KRONIG, hoogleraar in de afdeling der Technische Natuurkunde, voor een commissie uit de senaat te verdedigen op woensdag 19 april 1961 des namiddags te 4 uur

door

JOHN WILLIAM REYN

vliegtuigbouwkundig ingenieur
geboren te Hilversum

Druck der Universitätsdruckerei H. Stürtz AG., Würzburg

Dit proefschrift is goedgekeurd door de promotor Prof. Dr. R. Timman

Aan de nagedachtenis van mijn Vader
Aan mijn Moeder

Differential-geometric Considerations on the Hodograph Transformation for Irrotational Conical Flow

Contents

1. Introduction

This paper considers supersonic spatial flow fields which are conical in the sense originally introduced into aerodynamics by Busemann [*1*]. In such a flow the velocity and the conditions defining the state of the gas, *e.g.*, the pressure and temperature, are constant on rays through one point of the physical space, called the center of the conical field. Generalized conical flows, being flows in which these quantities are homogeneous of degree higher than zero (*e.g.* [*2*]), and conical fields used to construct flows of incompressible fluids (*e.g.* [*3*]) are thus excluded.

The treatment of conical flows within the frame of the linearized theory was initiated by Busemann [*4*] and has been given much attention since by many authors (*e.g.* [*5*] and [*6*]). Also, higher order approximations were considered, where either linear theory ([*7*], [*8*]) or the non-linear solution for the axially symmetric flow around a circular cone ([*9*], [*10*]) were chosen as a starting point.

For a long time the development of non-linear theory has been restricted to the study of particular examples, such as the solution for the axi-symmetric flow around a circular cone, given by BUSEMANN [*1*], [*11*] and by TAYLOR & MACCOLL [*12*], and other types of conical flow [*13*]. In the non-linear theory the flow around a specific body is obtained as a numerical solution of the differential equations. Methods of construction of such a numerical solution have been discussed by MASLEN [*14*], FOWELL [*15*] and FERRI, VAGLIO-LAURIN & NESS [*16*], [*17*]. However, in solutions found by these methods, for example for the flow around a flat delta wing with supersonic leading edges as given by MASLEN [*14*] and FOWELL [*15*], certain discrepancies arise. It is of interest therefore to consider in more detail the non-linear equations governing conical flow. This has been done by BULAKH in a number of papers [*18*]–[*22*], partly commenting on papers cited above [*21*], [*22*]. In the present paper the properties of non-linear isentropic conical flow are studied through a different approach, considering surface elements of integral surfaces of the non-linear equation from the point of view of differential geometry. For this purpose the hodograph transformation of isentropic conical flow, as studied first by BUSEMANN [*11*], [*23*] and later by GIESE [*24*], NIKOL'SKII [*25*] and RYZHOV [*26*], appears to be particularly useful.

2. Irrotational conical flow analyzed on the unit sphere around the center of the flow field

In the physical space let a right-handed co-ordinate system x, y, z be fixed with the origin at the center of the conical field, and let u, v and w be the components of the velocity along the axes, respectively. The coefficients of viscosity and heat conduction of the gas are assumed to be zero. If it is assumed moreover that the flow is isentropic, the three conservation laws (mass, momentum and energy) yield the following equation:

$$u_x\left(1-\frac{u^2}{a^2}\right)+v_y\left(1-\frac{v^2}{a^2}\right)+w_z\left(1-\frac{w^2}{a^2}\right)- \\ -\frac{u\,v}{a^2}(u_y+v_x)-\frac{v\,w}{a^2}(v_z+w_y)-\frac{u\,w}{a^2}(w_x+u_z)=0, \tag{1}$$

where a is the local velocity of sound, related to the velocity components by

$$a^2=\frac{\gamma+1}{2}a_*^2-\frac{\gamma-1}{2}(u^2+v^2+w^2)=\frac{\gamma+1}{2}a_*^2-\frac{\gamma-1}{2}q^2, \tag{2}$$

a_* is the critical velocity of sound, and γ is the ratio of specific heats $\left(\gamma=\frac{c_p}{c_v}\right)$.

If the flow is free of rotation, a velocity potential may be defined in the usual way such that

$$\varphi_x=u,\quad \varphi_y=v,\quad \varphi_z=w. \tag{3}$$

Equation (1) then becomes

$$\varphi_{xx}\left(1-\frac{u^2}{a^2}\right)+\varphi_{yy}\left(1-\frac{v^2}{a^2}\right)+\varphi_{zz}\left(1-\frac{w^2}{a^2}\right)- \\ -2\varphi_{xy}\frac{u\,v}{a^2}-2\varphi_{yz}\frac{v\,w}{a^2}-2\varphi_{xz}\frac{u\,w}{a^2}=0. \tag{4}$$

This equation may now be specialized for conical flow, using the property that the velocity does not change along rays through the center of the field. The velocity and the state of the gas depend therefore on two length co-ordinates instead of three, as in the general case of spatial flows. These co-ordinates may be taken arbitrarily to be x and y, and the flow may be considered in a plane $z=$ const. It is convenient also to analyze the flow on a unit sphere with center at the center of the conical field. The plane $z=1$ is then a plane tangent to this sphere at the point (0, 0, 1). By rotating the x, y, z axes, any point on the sphere can be taken as this point. The conical properties of the flow may be expressed by putting

$$\varphi = z\,F(\xi,\eta), \tag{5}$$

where $\xi = x/z$ and $\eta = y/z$, and from (3) then follows

$$u = F_\xi, \qquad v = F_\eta, \qquad w = F - \xi\,F_\xi - \eta\,F_\eta. \tag{6}$$

With the aid of (5) the following equation may be written for equation (4):

$$F_{\xi\xi}\left[1+\xi^2-\frac{(u-w\,\xi)^2}{a^2}\right]+2F_{\xi\eta}\left[\xi\,\eta-\frac{(u-w\,\xi)\,(v-w\,\eta)}{a^2}\right]+ \\ +F_{\eta\eta}\left[1+\eta^2-\frac{(v-w\,\eta)^2}{a^2}\right]=0. \tag{7}$$

In order to determine under what conditions this quasi-linear homogeneous partial differential equation is elliptic, parabolic or hyperbolic the characteristic directions may be determined from the equation

$$\left(\frac{d\eta}{d\xi}\right)^2_{\text{char.}}\left[1+\xi^2-\frac{(u-w\,\xi)^2}{a^2}\right]-2\left(\frac{d\eta}{d\xi}\right)_{\text{char.}}\left[\xi\,\eta-\frac{(u-w\,\xi)\,(v-w\,\eta)}{a^2}\right]+ \\ +\left[1+\eta^2-\frac{(v-w\,\eta)^2}{a^2}\right]=0. \tag{8}$$

For the local investigation of the flow it is convenient to use a co-ordinate system in which velocity components are measured along and perpendicular to the radius under consideration. The x, y and z axes are therefore rotated in such a way that the z axis has the direction of the radius under consideration and the x axis is in the direction of the velocity component perpendicular to the radius. The rotated system may be indicated by X, Y and Z, and the velocity components by U, V and W, respectively, U being the velocity component perpendicular to the radius and W the velocity component along the radius. If the flow is analyzed on the unit sphere, U is the velocity component tangent to the sphere. A streamline on the sphere may be defined as the intersection with a streamsurface, which may be constructed as a cone with the vertex at the center of the conical field and going through a spatial streamline. A streamline on the unit sphere is thus directed along the X axis or the velocity component U and is named a conical streamline. The characteristics given by (8) may be drawn on the unit sphere and are called the conical characteristics. For the point (0, 0, 1) in the X, Y, Z system the conical characteristic directions read

$$\left(\frac{d\Xi}{dH}\right)_{\text{char.}}=\frac{\pm 1}{\sqrt{\dfrac{U^2}{a^2}-1}}. \tag{9}$$

The conical characteristics thus subtend the Mach angle, defined in terms of the velocity on the surface of the unit sphere, with a conical streamline. Let us call this Mach angle the conical Mach angle μ_c and the Mach number defined in terms of the velocity U the conical Mach number $M_c(=U/a)$; then equation (9) can be written as

$$\left(\frac{d\Xi}{dH}\right)_{\text{char.}} = \frac{\pm 1}{\sqrt{M_c^2-1}} = \pm \tan \mu_c. \tag{10}$$

In analogy with two-dimensional plane flow the velocity normal to the conical characteristics is equal to the speed of sound. The conical characteristic directions are real and have two different values for $M_c > 1$; the equation is then of hyperbolic type, and the flow will be called conical-supersonic flow. For $M_c = 1$ the two conical characteristic directions are coincident, real and perpendicular to the conical streamline; the equation is parabolic, and the flow will be termed conical-sonic. If $M_c < 1$, the conical characteristic directions are imaginary; the equation is of elliptic type, and the flow will be called conical-subsonic flow. Points on the unit sphere where $U=0$ will be called conical stagnation points*. It is of interest to consider the relation between the characteristic surfaces in the spatial flow and the conical characteristics thus defined. A disturbance generated at a point of the flow field travels along the characteristic surface through that point; the characteristic surface starts as a characteristic or Mach cone. All characteristic surfaces emanating from points on the ray of the point considered may be constructed by a similarity transformation of the given characteristic surface with respect to the center of the conical field. The envelope of all characteristic surfaces so obtained is thus a conical surface, which intersects the unit sphere along the conical characteristics going through the point of intersection of the ray under consideration. This can be seen in the following way. Since the velocity component normal to the envelope, being a surface to which all characteristic surfaces are tangent, is equal to the velocity component normal to a characteristic surface, this velocity is sonic. Since the normal to the conical envelope is perpendicular to every curve on the envelope through the point considered, the normal at a point of intersection with the unit sphere also is perpendicular to the ray through that point and the intersection of the envelope with the unit sphere. The normal to the envelope thus is tangent to the unit sphere and perpendicular to the intersection of the envelope with the unit sphere; the velocity component along it is sonic, which shows that the intersections are conical characteristics. A conical disturbance may be defined as a disturbance generated with equal strength all along one ray. The conical characteristics are then the lines along which conical disturbances travel. An analogy with two-dimensional plane flow may be interpreted in the following sense. When a two-dimensional sound source is moving in a plane, the sound signals emitted by the source are propagated by sound waves which, if the velocity of the source is supersonic, form an envelope, being characteristics or Mach lines. In conical flow the disturbances travelling along the characteristic surfaces may be thought of as propagating on the unit sphere along curves which are the

---

* A disadvantage of this term is that the source-like character of a conical stagnation point ($U=0$, thus $W \neq 0$, because $q \neq 0$) is not expressed by it.

intersections of the characteristic surfaces with the unit sphere. When the flow is conical-supersonic, the curves of intersection belonging to the characteristic surfaces of one ray have an envelope which consists of conical characteristics on the sphere.

It may be noted that the characteristic surface emanating from the center of the conical field is of special interest. This surface coincides with the Mach cone with its apex at the center of the field and intersects the unit sphere along a conical-sonic line. This may be seen from the fact that a characteristic cone at some point of this conical characteristic surface is tangent to it along the radius through this point. The velocity component normal to the radius is therefore equal to the velocity component normal to the characteristic surface or Mach cone. Since the latter velocity component is sonic, the velocity component normal to the radius is sonic, and $M_c = 1$.

The velocity at the center of the conical field is in general multivalued; hence the Mach cone is not necessarily circular. Also it may be noticed that the influence of the center of the conical field is not restricted to the downstream interior of the characteristic cone from the center of the field. Actually it is confined to a cone, which may be constructed by connecting the center of the cone field with all points on the unit sphere by a curve formed by the conical characteristics which envelop the conical-sonic line. This may be seen in the spatial flow field by assuming that the disturbances originating in the center of the field travel initially over the conical characteristic surface from the center of the field. According to HUYGENS' principle each point reached on this surface in turn acts as a source of disturbances which propagate along the characteristic surface of that point. The latter surface is tangent to the conical characteristic surface from the origin but does not necessarily lie inside the downstream interior of it. The envelope of all characteristic surfaces starting at the characteristic surface from the center of the field thus bounds the region of influence of that center. This envelope intersects the unit sphere along the aforementioned curve.

In order to illustrate the quantities defined on the unit sphere, parallel flow throughout the physical space may be considered as an example of conical flow. The center of the field may be chosen arbitrarily at any point of the flow. The unit sphere is sketched in Fig. 1. The conical streamlines, being the intersections with the sphere of meridian planes through the diameter connecting the conical stagnation points, go from one conical stagnation point to the other. Conical-subsonic and conical-supersonic regions may be distinguished, separated by circular conical-sonic lines which are the intersections of the Mach cone from the center of the field with the sphere. The envelope of characteristic surfaces emanating from points of one radius consists of two planes which pass through this radius and are tangent to the Mach cone through the center of the field. The conical characteristics are the intersections of these planes with the sphere.

The difficulty in trying to determine the physical properties of conical flow lies partly in the fact that regions of conical-subsonic and conical-supersonic flow may occur simultaneously in a flow field, in which case (7) is of the mixed type. Since partial differential equations of the mixed type are in general difficult to handle, we use an approach which lends itself well to this specific problem.

The properties of conical flow are given by the states of motion that a gas particle in a conical flow might have.

The motion of a gas particle may be determined by its velocity, acceleration and higher derivatives of the velocity up to an arbitrary order. It is seen from equation (6) that when for a point on the unit sphere the velocity is given by its components along the axes, the co-ordinates of the integral surface $F(\xi, \eta)$ representing a flow where such a situation occurs and the tangent plane at some point on the surface are determined. Similarly, the magnitude and direction of the derivative of the velocity up to some order determines the surface element of F at that point, up to that order.

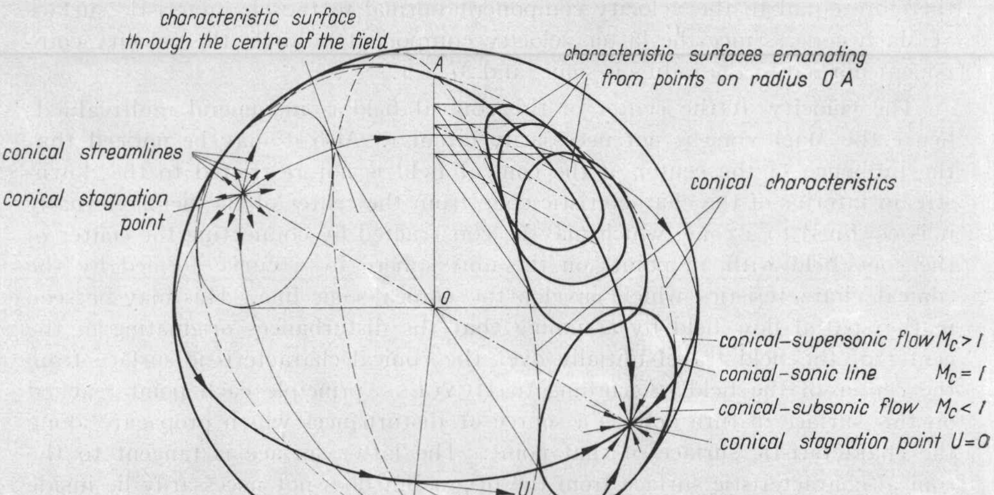

Fig. 1. Description on the unit sphere of parallel flow throughout physical space

To all geometrically possible surface elements that the differential equation permits to be surface elements of an integral surface thus correspond possible motions of a gas particle in a conical flow. The physics of conical flow is thus reduced to the differential geometry of integral surfaces of the differential equation for conical flow. In combination with (7), it is useful from the point of view of differential geometry to consider an equivalent equation obtained by the Legendre or hodograph transformation, which will now be discussed.

3. The hodograph transformation of irrotational conical flow

The hodograph transformation of irrotational conical flow is obtained in the usual way by introducing the Legendre potential

$$\chi(u, v) = u\,\xi + v\,\eta - F(\xi, \eta)\,, \tag{11}$$

so that

$$\chi_u = \xi\,, \quad \chi_v = \eta\,. \tag{12}$$

Comparing (6) and (11), we see that

$$\chi(u, v) = -\,w(u, v)\,. \tag{13}$$

The opposite of the velocity component along one axis may therefore serve as the Legendre potential, being a function of the other two velocity components, and the conical flow may be represented by a surface in the hodograph space.

By use of (13) in equation (12) follows

$$w_u = -\xi, \quad w_v = -\eta. \tag{14}$$

Differentiating (14) yields

$$\begin{aligned} d\xi &= -dw_u = -(w_{uu}\,du + w_{uv}\,dv), \\ d\eta &= -dw_v = -(w_{vu}\,du + w_{vv}\,dv). \end{aligned} \tag{15}$$

If the Jacobian determinant $\Delta \equiv w_{uu} w_{vv} - w_{uv}^2$ is finite and different from zero, (15) may be solved for du and dv, and we have

$$\begin{aligned} du &= \frac{1}{\Delta}(-w_{vv}\,d\xi + w_{uv}\,d\eta), \\ dv &= \frac{1}{\Delta}(w_{vu}\,d\xi - w_{uu}\,d\eta). \end{aligned} \tag{16}$$

The transformation is then locally one-to-one; that is, to one point on the unit sphere in the physical space corresponds one point on the surface in the hodograph space, and vice versa. Singularities in the transformation occur for $\Delta = 0$ or $\Delta \to \infty$. Furthermore, since

$$\begin{aligned} du &= u_\xi\,d\xi + u_\eta\,d\eta = F_{\xi\xi}\,d\xi + F_{\xi\eta}\,d\eta, \\ dv &= v_\xi\,d\xi + v_\eta\,d\eta = F_{\xi\eta}\,d\xi + F_{\eta\eta}\,d\eta, \end{aligned} \tag{17}$$

comparing this equation with (16) yields the second derivatives of F, and the following differential equation may be written instead of equation (7):

$$\begin{aligned} w_{uu}\left[1 + w_v^2 - \frac{(v + w\,w_v)^2}{a^2}\right] - 2w_{uv}\left[w_u w_v - \frac{(u + w\,w_u)(v + w\,w_v)}{a^2}\right] + \\ + w_{vv}\left[1 + w_u^2 - \frac{(u + w\,w_u)^2}{a^2}\right] = 0. \end{aligned} \tag{18}$$

It may be noted that if $w(u, v)$ is a solution of this equation satisfying given boundary conditions, $-w(-u, -v)$ is also a solution. Therefore, as in all isentropic flows subject to boundary conditions in the form of prescribed streamlines, the flow may be reversed. The significance of this fact will be discussed later in relation to the limit cones.

Equation (18) is of the same type as (7), and the characteristics of the equation may be written as

$$\begin{aligned} \left(\frac{dv}{du}\right)_{\text{char.}}^2 \left[1 + w_v^2 - \frac{(v + w\,w_v)^2}{a^2}\right] + 2\left(\frac{dv}{du}\right)_{\text{char.}} \left[w_u w_v - \frac{(u + w\,w_u)(v + w\,w_v)}{a^2}\right] + \\ + \left[1 + w_u^2 - \frac{(u + w\,w_u)^2}{a^2}\right] = 0. \end{aligned} \tag{19}$$

For the conical characteristic directions on the hodograph surface in the U, V and W co-ordinates we have

$$\left(\frac{dV}{dU}\right)_{\text{char.}} = \pm\sqrt{M_c^2 - 1}. \tag{20}$$

Elliptic and hyperbolic regions again may be distinguished on the hodograph surface, having two different imaginary and real conical characteristic directions, respectively, and corresponding to conical-subsonic and conical-supersonic flow. If the flow is conical-sonic, the two conical characteristic directions coincide along the U axis.

As in two-dimensional plane flow the velocity along the conical characteristics on the hodograph surface is sonic. The angle between the velocity vector q and a conical characteristic on the hodograph surface is therefore the angle α, defined from the local Mach number $M (M = q/a)$ and given by

$$\tan \alpha = \pm \sqrt{M^2 - 1} . \tag{21}$$

It is equal to the angle between the velocity vector q and the characteristics in the hodograph plane for two-dimensional plane flow, which are the well-known Prandtl-Meyer epicycloids. Thus, when a cone passing through a conical characteristic on the hodograph surface and having its vertex at the origin of the hodograph space is developed onto a plane, a Prandtl-Meyer epicycloid is obtained [*24*].

4. Differential-geometric description of the hodograph transformation for irrotational conical flow

From (14) it follows that the radius in the physical space is perpendicular to the surface element at the corresponding point on the hodograph surface. The sphere obtained by collecting at one point the unit vectors along the normals to the hodograph surface is the unit sphere in the physical space, as discussed before. *From differential geometry the transformation from the hodograph space to the physical space may be recognized as being the spherical or Gaussian transformation of the hodograph surface.*

An analysis of the geometry of the hodograph surface may start by investigating the properties of its curvature. If further exploration is of interest, third and higher derivatives may also be taken into consideration.

A study of the curvature of the hodograph surface can be based upon Dupin's indicatrix. Dupin's indicatrix is formed by laying out along the normal sections of the surface distances equal to the square root of the absolute value of the radius of curvature of those sections. A curve related to Dupin's indicatrix is obtained as the intersection with the hodograph surface of a plane parallel to the tangent plane at the point under consideration at a distance C such that higher order derivatives may be neglected with respect to the second order derivatives when the shape of the curve of intersection is determined. If the second derivatives are continuous, a Taylor expansion yields the following equation for this intersection in the U, V, W system, attached to a radius for which $U = U_1$ and $W = W_1$:

$$\begin{gathered} W = W_1 - C , \\ W_{UU_1}(U - U_1)^2 + 2 W_{UV_1}(U - U_1)\, V + W_{VV_1} V^2 - 2C = 0 . \end{gathered} \tag{22}$$

This is a conic*, being an ellipse when $(W_{UU} W_{VV} - W_{UV}^2)_1 \equiv K_{G_1} > 0$, a hyperbola when $K_{G_1} < 0$ and a parabola degenerated into two parallel lines for $K_{G_1} = 0$.

---

* Dupin's indicatrix is similar to this conic for elliptic and parabolic points. For hyperbolic points Dupin's indicatrix consists in two conjugate hyperbolas, which are similar to this conic if C is given two equal and opposite values.

Points on the surface are called elliptic, hyperbolic and parabolic points, respectively. For an elliptic point the surface is curved in the same sense in all directions; for a parabolic point the same is true, while in one direction the curvature of the surface is zero; and for a hyperbolic point curvatures of the surface of opposite signs occur. For a hyperbolic point there are two directions for which the curvature of the surface becomes zero.

The axes of the conic are in the principal directions, and the corresponding radii of curvature are called the principal radii of curvature ϱ_1 and ϱ_2. Throughout this paper ϱ_1 will be chosen as the major principal radius of curvature and ϱ_2 as the minor principal radius of curvature. The principal directions are given by the angle $\alpha_{1,2}$ with respect to the U axis ($\alpha_{1,2}$ measured positive in counter-clockwise direction), where $\alpha_{1,2}$ may be deduced from

$$\tan 2\alpha_{1,2} = \frac{2W_{UV}}{W_{UU} - W_{VV}}. \tag{23}$$

Lines on the surface which at each point are tangent to one of the principal directions are called lines of curvature. The radius of curvature of the curve of intersection of a plane through the normal to the surface and making an angle $\bar{\alpha}$ with the major principal direction is given by EULER'S theorem,

$$\frac{1}{R} = \frac{1}{\varrho_1}\cos^2\bar{\alpha} + \frac{1}{\varrho_2}\sin^2\bar{\alpha}, \tag{24}$$

or in the U, V, W system,

$$-\frac{1}{R} = W_{UU}\cos^2\alpha + 2W_{UV}\sin\alpha\cos\alpha + W_{VV}\sin^2\alpha, \tag{25}$$

where α is the angle with respect to the U axis.

The normal curvature $\varkappa_n$ of a curve on the hodograph surface is the opposite of this value, whereas the other intrinsic second-order parameter of a curve on a surface, the geodesic torsion, may be expressed as

$$\tau_g = W_{UV}\cos^2\alpha - (W_{UU} - W_{VV})\sin\alpha\cos\alpha - W_{UV}\sin^2\alpha, \tag{26}$$

where τ_g is positive if the normal to the surface turns to the right when moving along the curve.

From (23) and (26) it then follows that the geodesic torsions of the lines of curvature are equal to zero. If transformed to the unit sphere, the lines of curvature have the same direction there as on the hodograph surface.

The ratio of corresponding line elements along the lines of curvature on the unit sphere and the hodograph surface may be obtained from (15); the result is the Rodrigues equations

$$(d s_{1,2})_h = \varrho_{1,2}(d s_{1,2})_{ph}, \tag{27}$$

where ϱ_1 and ϱ_2 are the radii of curvature in the principal directions 1 and 2, respectively, and the indices h and ph refer to the hodograph surface and to the unit sphere in the physical space, respectively.

A direction making an angle α_h with principal direction 1 on the hodograph surface (α_h being measured positive in the counter-clockwise direction) makes the angle α_{ph} with the direction corresponding to principal direction 1 on the unit sphere. From (27) these angles are related by

$$\tan\alpha_{ph} = \frac{\varrho_1}{\varrho_2}\tan\alpha_h. \tag{28}$$

The area of a surface element dA_{ph} on the unit sphere and the area of the corresponding surface element on the hodograph surface dA_h are connected with the Gaussian curvature K_G by the relation

$$\frac{dA_{ph}}{dA_h} = \frac{1}{\varrho_1 \varrho_2} = K_G. \tag{29}$$

Since

$$K_G = W_{UU} W_{VV} - W_{UV}^2 = \Delta, \tag{30}$$

the Gaussian curvature or the Jacobian determinant is thus seen to be equal to the ratio of magnitudes of corresponding surface elements, being positive for an elliptic point, zero for a parabolic point and negative for a hyperbolic point. In relation to equation (28) it may be deduced that the image on the unit sphere of a closed curve on the hodograph surface is traversed in the same sense as the curve on this surface if $K_G > 0$, and in the opposite sense if $K_G < 0$. Singularities in the transformation are to be expected for $K_G = 0$ and $K_G \to \infty$ ($\Delta = 0$ and $\Delta \to \infty$).

In addition to the Gaussian curvature, the mean curvature may be defined as the sum of the principal curvatures and given by

$$K_M = \frac{1}{\varrho_1} + \frac{1}{\varrho_2} = -(W_{UU} + W_{VV}), \tag{31}$$

where ϱ_1 and ϱ_2 are chosen to be positive if the hodograph surface is convex towards the direction of the positive W axis.

Other directions of interest are conjugate directions. The directions defined by the angles α_h and α_h' are said to be conjugate if

$$\tan \alpha_h \tan \alpha_h' = -\frac{\varrho_2}{\varrho_1},$$

or

$$W_{UU} + W_{UV}\{\tan(\alpha_1 + \alpha_h) + \tan(\alpha_1 + \alpha_h')\} + W_{VV} \tan(\alpha_1 + \alpha_h) \tan(\alpha_1 + \alpha_h') = 0. \tag{32}$$

By use of (28), equation (32) may be written as

$$\tan \alpha_h' \tan \alpha_{ph} = -1. \tag{33}$$

The image on the unit sphere in physical space of a direction on the hodograph surface is therefore perpendicular to its conjugate direction on the hodograph surface.

Directions which are self-conjugate are asymptotic directions, which transform perpendicularly to their images. They may be obtained from (22) or (32):

$$\left(\frac{dV}{dU}\right)_{\text{asympt.}} = \frac{-W_{UV} \pm \sqrt{-(W_{UU} W_{VV} - W_{UV}^2)}}{W_{VV}}. \tag{34}$$

Thus for an elliptic point ($K_G > 0$) the asymptotic directions are imaginary; for a hyperbolic point ($K_G < 0$) there are two real asymptotic directions; and for a parabolic point ($K_G = 0$) the two real asymptotic directions coincide along the axis of the parabola, which is in the principal direction where $\varrho \to \infty$.

The differential-geometric properties of a surface, thus summarized, may be used to express the physical quantities of interest in terms of geometrical properties of the hodograph surface, which is the particular surface under consideration. This surface is characterized by differential equation (18), which at a point of the surface, since $W_U = W_V = 0$, yields the relation

$$W_{UU} + W_{VV}(1 - M_c^2) = 0, \tag{35}$$

first given by BUSEMANN [*23*]. The radii of curvature R_U and R_V in the directions of the U and V axis, respectively, then satisfy the equation

$$R_U(1 - M_c^2) + R_V = 0. \tag{36}$$

From (35), (20) and (32) it may easily be seen that the conical characteristics on the hodograph surface form a conjugate net. The conical characteristics on the unit sphere of one family are therefore perpendicular to the conical characteristics on the hodograph surface of the other family. The $+(-)$ sign in equation (10) corresponds to the $+(-)$ sign in (20), and the same situation is encountered as in two-dimensional plane flow, as has been shown by GIESE [*24*] and RYZHOV [*26*]*.

Another system of conjugate directions is formed by the streamlines on the hodograph surface and the lines of constant speed (or a, p and M are constant). Partial differentiation of

$$q^2 = u^2 + v^2 + w^2 \tag{37}$$

with respect to v, for a point $X = Y = 0$, yields

$$\frac{\partial q}{\partial V} = 0. \tag{38}$$

The lines $q =$ constant on the hodograph surface therefore intersect the U axis perpendicularly and are thus perpendicular to the conical streamline on the unit sphere. Furthermore, the lines $q =$ constant on the unit sphere are normal to the acceleration, which has the same direction as the conical hodograph streamline. The streamlines and the lines $q =$ constant therefore form a conjugate system on the hodograph surface. Further it is seen that the lines $q =$ const. bisect the angle between the conical characteristics on that surface [*24*]. The variations of q, a and M are found by partial differentiation with respect to u of equations (2) and (37). For a point $X = Y = 0$

$$\frac{dq}{dU} = \frac{\partial q}{\partial U} = \frac{M_c}{M}, \tag{39}$$

$$\frac{da}{dU} = \frac{\partial a}{\partial U} = -\frac{\gamma - 1}{2} M_c, \tag{40}$$

$$\frac{dM}{dU} = \frac{\partial M}{\partial U} = \frac{M_c}{q}\left(1 + \frac{\gamma - 1}{2} M_c^2\right). \tag{41}$$

The variations of the velocity component normal to the radius U_n and of M_c are also of interest. For a point $X = Y = 0$ it can be shown, after some calculation, that

$$\frac{\partial U_n}{\partial U} = 1 + W W_{UU}, \tag{42a}$$

$$\frac{\partial U_n}{\partial V} = W W_{UV}, \tag{42b}$$

* See also [*28*], p. 483, note 9.

and

$$\frac{\partial M_c}{\partial U} = \frac{1}{a}\left[1 + \frac{\gamma-1}{2} M_c^2 + W W_{UU}\right], \tag{43a}$$

$$\frac{\partial M_c}{\partial V} = \frac{1}{a} W W_{UV}, \tag{43b}$$

from which the direction of a line $M_c =$ constant is found to be given by

$$\left(\frac{dV}{dU}\right)_{M_c=\text{const.}} = -\frac{1 + \frac{\gamma-1}{2} M_c^2 + W W_{UU}}{W W_{UV}}. \tag{44}$$

The direction of the conical streamline on the hodograph surface, which also is the direction of the acceleration, may be seen from (32) and (38) to satisfy

$$\tan\beta = \left(\frac{dV}{dU}\right)_s = -\frac{W_{UV}}{W_{VV}}. \tag{45}$$

The magnitude of the acceleration along a streamline in the physical space may be expressed in terms of the curvatures of the hodograph surface in the following way. Along a streamline in the physical space

$$\left(\frac{dx}{dz}\right)_s = \frac{u}{w}, \quad \text{and} \quad \left(\frac{dy}{dz}\right)_s = \frac{v}{w}, \tag{46}$$

where the index s refers to conditions along the streamline. By differentiation of (14) we have

$$\begin{aligned}(dx)_s &= -w_u (dz)_s - z (dw_u)_s, \\ (dy)_s &= -w_v (dz)_s - z (dw_v)_s.\end{aligned} \tag{47}$$

or from equation (46)

$$(dx)_s = \frac{-z\left[w_{uu}(du)_s + w_{uv}(dv)_s\right]}{1 + w_u \frac{w}{u}}, \tag{48}$$

$$(dy)_s = \frac{-z\left[w_{uv}(du)_s + w_{vv}(dv)_s\right]}{1 + w_v \frac{w}{v}}. \tag{49}$$

Again using (46) leads to*

$$\left(\frac{dv}{du}\right)_s = \frac{(v + w w_v)\, w_{uu} - (u + w w_u)\, w_{uv}}{(u + w w_u)\, w_{vv} - (v + w w_v)\, w_{uv}}, \tag{50}$$

and

$$\begin{aligned}(dx)_s &= -z u \frac{w_{uu} w_{vv} - w_{uv}^2}{(u + w w_u)\, w_{vv} - (v + w w_v)\, w_{uv}} (du)_s, \\ (dy)_s &= -z v \frac{w_{uu} w_{vv} - w_{uv}^2}{(u + w w_u)\, w_{vv} - (v + w w_v)\, w_{uv}} (du)_s, \\ (dz)_s &= -z w \frac{w_{uu} w_{vv} - w_{uv}^2}{(u + w w_u)\, w_{vv} - (v + w w_v)\, w_{uv}} (du)_s.\end{aligned} \tag{51}$$

For the u component then follows

$$\left(\frac{du}{ds}\right)_s = -\frac{1}{q z} \frac{(u + w w_u)\, w_{vv} - (v + w w_v)\, w_{uv}}{w_{uu} w_{vv} - w_{uv}^2}, \tag{52}$$

* Equation (50) may be used as a check on (45).

and for the v component

$$\left(\frac{dv}{ds}\right)_s = -\frac{1}{qz}\,\frac{(v+w\,w_v)\,w_{uu}-(u+w\,w_u)\,w_{uv}}{w_{uu}\,w_{vv}-w_{uv}^2}. \tag{53}$$

Furthermore,

$$\left(\frac{dw}{ds}\right)_s = \left(\frac{du}{ds}\right)_s w_u + \left(\frac{dv}{ds}\right)_s w_v, \tag{54}$$

so that from equations (52)—(54) follows

$$\left(\frac{dw}{ds}\right)_s = -\frac{1}{qz}\,\frac{(u+w\,w_u)\,(w_u\,w_{vv}-w_v\,w_{uv})-(v+w\,w_v)\,(w_u\,w_{uv}-w_v\,w_{uu})}{w_{uu}\,w_{vv}-w_{uv}^2}. \tag{55}$$

By use of the relation

$$q\left(\frac{dq}{ds}\right)_s = u\left(\frac{du}{ds}\right)_s + v\left(\frac{dv}{ds}\right)_s + w\left(\frac{dw}{ds}\right)_s, \tag{56}$$

and of equations (52), (53) and (55) the acceleration along the streamline is then found to be

$$\frac{dq}{dt} = q\left(\frac{dq}{ds}\right)_s = -\frac{1}{qz}\,\frac{(v+w\,w_v)^2\,w_{uu}-2\,(u+w\,w_u)\,(v+w\,w_v)\,w_{uv}+(u+w\,w_u)^2\,w_{vv}}{w_{uu}\,w_{vv}-w_{uv}^2}, \tag{57}$$

or, by (18)

$$\frac{dq}{dt} = -\frac{a^2}{qz}\,\frac{(1+w_v^2)\,w_{uu}-2w_u\,w_v\,w_{uv}+(1+w_u^2)\,w_{vv}}{w_{uu}\,w_{vv}-w_{uv}^2}. \tag{58}$$

In the U, V, W co-ordinate system (58) reads at the point under consideration

$$\frac{dq}{dt} = -\frac{a^2}{q\,r}\,\frac{W_{UU}+W_{VV}}{W_{UU}\,W_{VV}-W_{UV}^2}, \tag{59}$$

where r is the distance measured along the radius. When (30) and (31) are used, the acceleration along the physical streamline becomes

$$g_s = \frac{a}{M\,r}\,\frac{K_M}{K_G} = \frac{a}{M\,r}\,(\varrho_1+\varrho_2). \tag{60}$$

This acceleration is therefore seen to be simply related to the principal radii of curvature of the hodograph surface.

From this result the pressure gradient along the streamline may be found:

$$\frac{dp}{ds} = -\frac{\varrho\,a}{M\,r}\,\frac{K_M}{K_G} = -\frac{\varrho\,a}{M\,r}\,(\varrho_1+\varrho_2), \tag{61}$$

where ϱ is the density. The acceleration normal to the streamline may be derived from equation (45) and (60):

$$g_n = \frac{a}{M\,r}\,|\varrho_1+\varrho_2|\,\sqrt{\frac{M^2}{M_c^2}\left(1+\frac{W_{UV}^2}{W_{VV}^2}\right)-1}. \tag{62}$$

From this result follows the radius of curvature of the streamline in the physical space:

$$R = \frac{a\,M^3\,r}{|\varrho_1+\varrho_2|}\,\frac{1}{\sqrt{\frac{M^2}{M_c^2}\left(1+\frac{W_{UV}^2}{W_{VV}^2}\right)-1}}. \tag{63}$$

5. Analysis of the hodograph surface when the transformation is regular

Once the co-ordinates at a point of the hodograph surface are given by the velocity q and the tangent plane at that point by the direction of the normal, the geometry of the surface may be further specified by the curvature, given by the

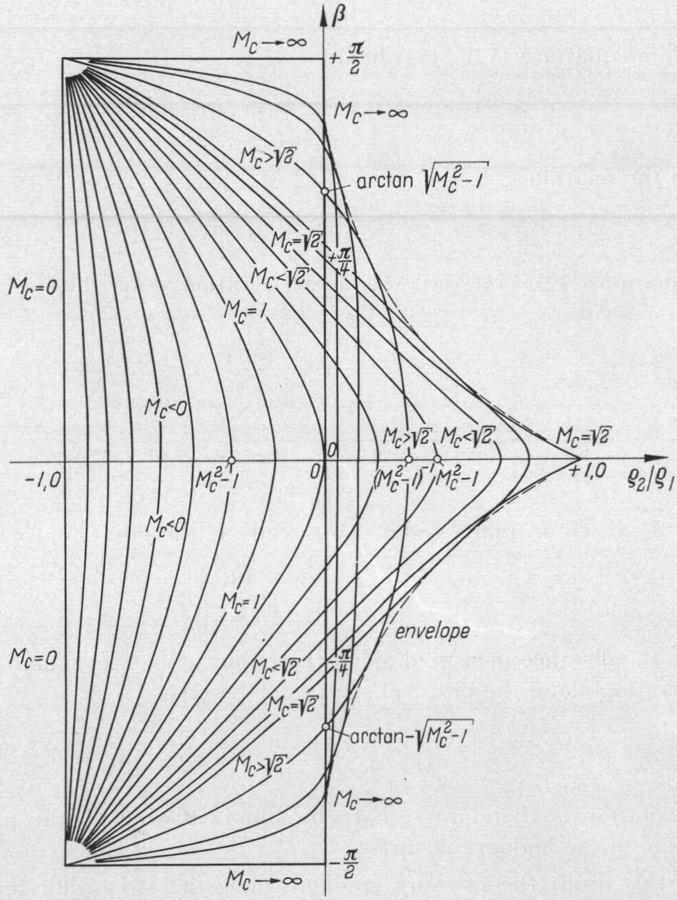

Fig. 2a. Direction of the conical hodograph streamline

value of the three second derivatives. The hodograph surface is described by the differential equation (18), which yields one relation for the second derivatives in two perpendicular directions, *i.e.* (35). Two additional data are then required to determine a surface element to the second order. For these it will be convenient to choose ϱ_2/ϱ_1 and $\varrho_1+\varrho_2$. In addition the sign of α_1 must be given, since without loss of generality α_1 may be chosen in the interval between $-\frac{\pi}{2}$ and $\frac{\pi}{2}$. When the velocity q and the tangent plane (determined by the direction of the normal or the radius in the physical space) are given, the value of M_c is fixed. It may then be asked how ϱ_2/ϱ_1 and $\varrho_1+\varrho_2$ determine the surface. For a given value of M_c, the directions of the characteristics are determined, and since they are conjugate, to every value of ϱ_2/ϱ_1 corresponds one value of the angle of the major axis α_1 of the given sign. Thence follows also one value of β giving the direction of the conical hodograph streamline (or the acceleration), since it is the direction conjugate to the direction of the V axis.

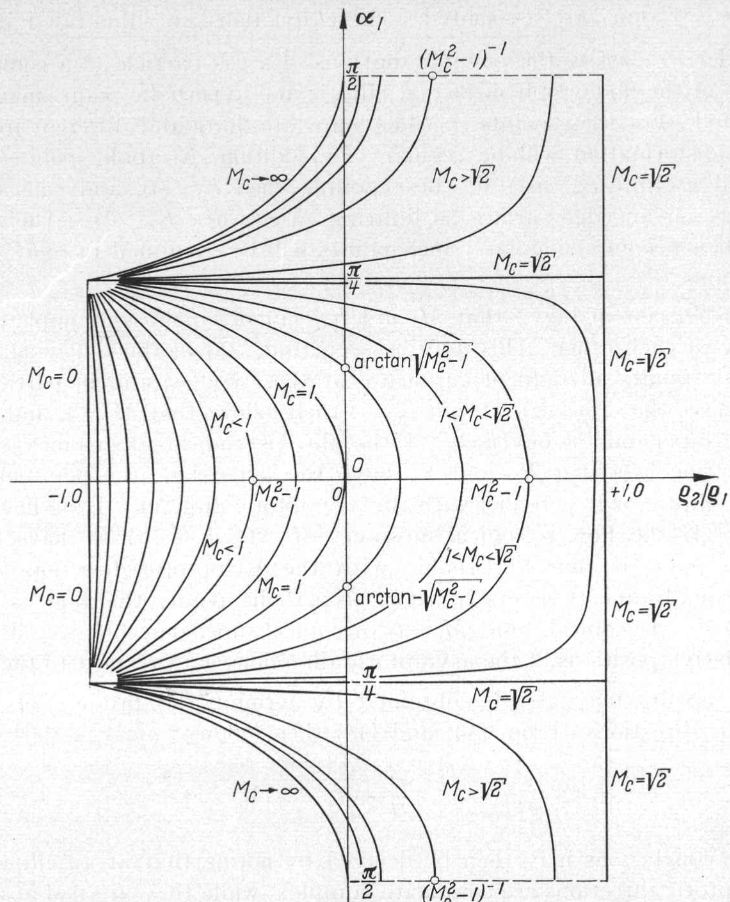

Fig. 2b. Direction of the major principal axis at a point of the hodograph surface

The parameters M_c and ϱ_2/ϱ_1 therefore determine α_1 and β. The parameter $\varrho_1+\varrho_2$ may be seen from (60) and (62) to determine the magnitude of the acceleration and can be varied independently of ϱ_2/ϱ_1★.

With the aid of (20), (23), (32), (35) and (45) the following relations may then be derived for α_1 and β:

$$\tan\alpha_1 = \pm\sqrt{\frac{M_c^2-1-\dfrac{\varrho_2}{\varrho_1}}{1-\dfrac{\varrho_2}{\varrho_1}(M_c^2-1)}}\,, \tag{64}$$

★ Except when $\varrho_1+\varrho_2=0$; then $\varrho_2/\varrho_1=-1$.

and

$$\tan\beta = \frac{\pm\sqrt{\left\{1-\frac{\varrho_2}{\varrho_1}(M_c^2-1)\right\}\left\{M_c^2-1-\frac{\varrho_2}{\varrho_1}\right\}}}{1+\frac{\varrho_2}{\varrho_1}}, \tag{65}$$

where the $\pm$ signs are associated. These functions are illustrated in Fig. 2.

In order to classify the possible motions of a gas particle in a conical flow, the shape of the hodograph surface at elliptic and hyperbolic points may now be investigated. For these points the Jacobians are finite and different from zero, so the transformation will be regular. In addition, parabolic points may be considered as limiting cases of these points when $K_G \to 0$, and conical points and points on an edge surface as limiting cases when $K_G \to \infty$. The transformation then becomes singular. Such points will be examined in more detail in later sections.

It can be seen in Fig. 2 that M_c and K_G cannot be chosen completely independently of each other. This may be seen from (35) in the following manner. For elliptic points all radii of curvature at these points, and in particular R_U and R_V, have the same sign. From (35) it then follows that $M_c > 1$, and the flow is conical-supersonic. Conversely, if the flow is conical-supersonic, it follows from equation (35) that R_U and R_V have the same sign; the point may then be either elliptic or hyperbolic, with the asymptotic directions lying in the same quadrant. If the flow is conical-subsonic ($M_c < 1$), R_U and R_V have opposite signs, the point is thus hyperbolic, with the asymptotic directions lying in different quadrants. Conversely, at a hyperbolic point, the flow is conical-subsonic ($M_c < 1$), conical-sonic ($M_c = 1$) or conical-supersonic ($M_c > 1$), depending on the relative positions of the asymptotic directions with respect to the U axis.

These results may also be obtained by forming the product of the two asymptotic directions. From (34) and (35) then follows*

$$\left(\frac{dV}{dU}\right)_{\text{asymp. 1}} \cdot \left(\frac{dV}{dU}\right)_{\text{asymp. 2}} = M_c^2 - 1. \tag{66}$$

The same conclusions may then be derived by noting that at an elliptic point the asymptotic directions are conjugate complex, while they are real at a hyperbolic point.

α) Conical-subsonic flow

Consider first conical stagnation points. At such a point $U=0$ and $M_c=0$, if $a \neq 0$ (M is finite). From (35) it follows that $W_{UU}+W_{VV}=0$; thus the curve given by (22) for $\pm C$ consists of two conjugate orthogonal hyperbolas, which are similar to DUPIN's indicatrix. From Fig. 2 it can be seen that β may have any value, so at the stagnation point conical streamlines from all directions can come together. This may also be concluded by remarking that at the point itself the direction of the U axis cannot be defined, since $U=0$. For the same

* With the aid of equations (20) and (66) the following property may be derived:

$$\left(\frac{dV}{dU}\right)_{\text{asymp. 1}} \cdot \left(\frac{dV}{dU}\right)_{\text{asymp. 2}} + \left(\frac{dV}{dU}\right)_{\text{char. 1}} \cdot \left(\frac{dV}{dU}\right)_{\text{char. 2}} = 0. \tag{66a}$$

reasons the directions of the principal axes can also have any value. Since $\varrho_2/\varrho_1 = -1$, the acceleration along the streamline, as given by (60), is zero, since $M \neq 0$. This result can be seen immediately by noting that the streamline falls along the radius through that point.

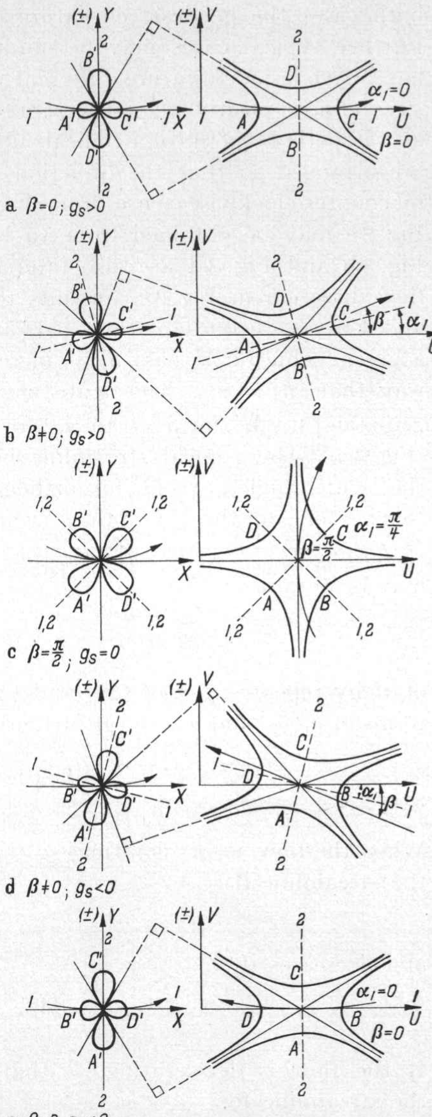

Fig. 3a—e. Typical conditions at a hyperbolic point of a conical-subsonic flow

Conversely, an orthogonal hyperbolic point does not necessarily represent a conical stagnation point. If the point is orthogonal hyperbolic, $\varrho_2/\varrho_1 = -1$, and the acceleration along the streamline is zero. The direction of the conical hodograph streamline is therefore perpendicular to the U axis $\left(\beta = \pm\frac{\pi}{2}\right)$. The conical streamline thus becomes perpendicular to its image, and the V axis therefore coincides with an asymptote. The U axis is then also an asymptote; thus $W_{UU} = W_{VV} = 0$. From (35) it then follows that the conical Mach number M_c may take any value, while for $M_c \neq 0$ the principal directions bisect the angles between the U and V axes $\left(\alpha_1 = \pm\frac{\pi}{4}\right)$. From equation (28) it is seen that at an orthogonal hyperbolic point the transformation becomes conformal.

For conical-subsonic flow ($M_c < 1$) points on the hodograph surface are hyperbolic. From BUSEMANN's relation, equation (35), it follows that for $\alpha_1 = 0$, ϱ_2/ϱ_1 has the value $M_c^2 - 1$. Since the physical conical streamline falls along a principal direction, the hodograph conical streamline also does so and is therefore along the U axis; thus $\beta = 0$. The acute angle between the asymptotes is bisected by the U axis. The situation is sketched in Fig. 3a for accelerating flow and in Fig. 3e for decelerating flow. According to (60), for accelerating flow $\varrho_1 + \varrho_2 > 0$, and, since $|\varrho_1| > |\varrho_2|$, it follows that $\varrho_1 > 0$ and $\varrho_2 < 0$. From the equations of RODRIGUES, equation (27), it may be deduced that points on DUPIN's indicatrix $ABCD$ are mapped onto a figure $A'B'C'D'$ on the unit sphere which is compressed in the direction of AC and stretched in the direction of BD. The images of points in the directions of the asymptotes coincide with the image of the point considered. The figure is then turned over along the major axis AC. For decelerating flow $\varrho_1+\varrho_2<0$ and since $|\varrho_1|>|\varrho_2|$, it follows that $\varrho_1<0$ and $\varrho_2>0$. Dupin's indicatrix $ABCD$ is than compressed and stretched in the same manner, but turned over along the minor axis AC. In both cases the geodesic curvature of the physical conical streamline is zero. Further typical cases may be obtained when the physical conical streamline has a geodesic curvature different from zero and the acceleration along the streamline is positive, equal to zero or negative, respectively. Typical conditions at a hyperbolic point of a conical-subsonic flow are given in Fig. 3. The sketches are arranged so that the direction of the conical hodograph streamline turns in counter-clockwise sense from Fig. 3a to Fig. 3e. It may be noticed that Fig. 3e may be obtained from 3a by reversing the direction of flow, whereas Fig. 3b and Fig. 3d are also interchangeable in that manner. Reversing the flow direction in Fig. 3c amounts to changing the direction of the positive Y and V axes. From equations (64) and (65) and Fig. 2 it may be seen that for a given value of M_c, as $|\beta|$ is increased from zero on, $|\alpha_1|$ changes in such a way that $|\beta|>|\alpha_1|$. The acute angle between the asymptotes oscillates from $2\arctan\sqrt{1-M_c^2}$ for $\beta=0$ to $\pi/2$ for an orthogonal hyperbolic point $(|\beta|=\pi/2)$ (Fig. 3c). The conical streamline lies between the asymptotes which enclose the acute angle, except for orthogonal hyperbolic points, in which cases it touches one of the asymptotes, which then subtend an angle of $\pi/2$ radians.

From (43a), (43b) and (45) the variation of M_c along a conical streamline may be obtained:

$$\left(\frac{dM_c}{dU}\right)_s=\frac{1}{a}\left[1+\frac{\gamma-1}{2}M_c^2+W\frac{K_G}{W_{VV}}\right],$$

or if by repeated use of (25) and (26) the second derivatives are expressed in terms of ϱ_1, ϱ_2 and α_1, and if furthermore (64) and (60) are used, we have

$$\left(\frac{dM_c}{dU}\right)_s=\frac{1}{a}\left[1+M_c^2\left\{\frac{\gamma-1}{2}-\frac{W a}{M r}\frac{1}{g_s}\right\}\right]. \tag{67}$$

When the flow is accelerating, so that $g_s>0$, it follows that M_c increases along the streamline if

$$W<\left(1+\frac{\gamma-1}{2}M_c^2\right)\frac{M r}{M_c^2 a}g_s$$

and decreases if

$$W>\left(1+\frac{\gamma-1}{2}M_c^2\right)\frac{M r}{M_c^2 a}g_s.$$

If the flow is decelerating, so that $g_s<0$, it follows that M_c increases along the streamline for

$$W>\left(1+\frac{\gamma-1}{2}M_c^2\right)\frac{M r}{M_c^2 a}g_s$$

and decreases for

$$W<\left(1+\frac{\gamma-1}{2}M_c^2\right)\frac{M r}{M_c^2 a}g_s.$$

The conical streamline is tangent to a line of constant M_c for

$$W=\left(1+\frac{\gamma-1}{2}M_c^2\right)\frac{M r}{M_c^2 a}g_s.$$

When the acceleration is equal to zero, (43b) shows that along the conical streamline M_c again may either increase, decrease or remain stationary. For comparison it may be noted that for two-dimensional plane flow the Mach number increases in expanding flow, decreases in compressing flow and does not change if the pressure does not vary along the streamline.

β) Conical-sonic flow

At a hyperbolic point the flow can also be conical-sonic ($M_c=1$). From BUSEMANN's relation, equation (35), it follows that if $M_c=1$ and $W_{VV}\neq 0$, then $W_{UU}=0$. One of the asymptotes of DUPIN's indicatrix thus falls along the U axis. The other asymptote falls in the first (and third) quadrant for $\alpha_1>0$ and in the second (and fourth) quadrant for $\alpha_1<0$. The angle of the major principal axis α_1 and the angle of the conical hodograph streamline β are seen from (64) and (65) to satisfy the relations

$$\tan\alpha_1=\pm\sqrt{-\frac{\varrho_2}{\varrho_1}}, \tag{68}$$

and

$$\tan\beta=\pm\frac{\sqrt{-\frac{\varrho_2}{\varrho_1}}}{1+\frac{\varrho_2}{\varrho_1}}. \tag{69}$$

These relations are illustrated in the curve for $M_c=1$ in Fig. 2. It may be deduced from equations (68) and (69) that if $|\beta|$ is increased from zero onward, $|\alpha_1|$ increases in such a way that $2|\alpha_1|>|\beta|>|\alpha_1|$. The acute angle between the asymptotes equals $2|\alpha_1|$ and increases from zero to $\pi/2$ when $|\beta|$ increases from zero to $\pi/2$, while $|\alpha_1|$ increases from zero to $\pi/4$. The conditions which may be encountered at a hyperbolic point if the flow is conical-sonic are similar to those in conical-subsonic flow, except that the case $\beta=0$ cannot occur. This leaves three typical conditions, all with a curved conical physical streamline and positive, zero and negative acceleration along the streamline, respectively. They are sketched in Fig. 4. The case $\beta=\pm\frac{\pi}{2}$, $\alpha=\pm\frac{\pi}{4}$ again corresponds to an orthogonal hyperbolic point; thus $W_{VV}=0$, and the acceleration along the streamline is equal to zero. It may be noted again that by reversing the direction of flow, Figs. 4a and 4c are interchangeable. It can further be shown that at a direction on the unit sphere perpendicular to the physical conical streamline the flow is conical-subsonic on the convex side of the streamline and conical-supersonic on the concave side. This direction, in fact, coincides with the Y axis and maps onto the U axis, since the latter is an asymptote and thus transforms perpendicularly to itself. On the Y axis the pressure on the convex side of the streamline is higher than on the concave side; the velocity gradient is therefore in the direction from the convex side to the concave side of the streamline. From (39) it follows that U increases when q increases; thus U increases from the convex side to the concave side. From (43a) it may be seen that then M_c also increases. The conical-subsonic flow is thus on the convex side, and the conical-supersonic flow region is on the concave side of the conical streamline. The positive U direction corresponds to the Y direction on the

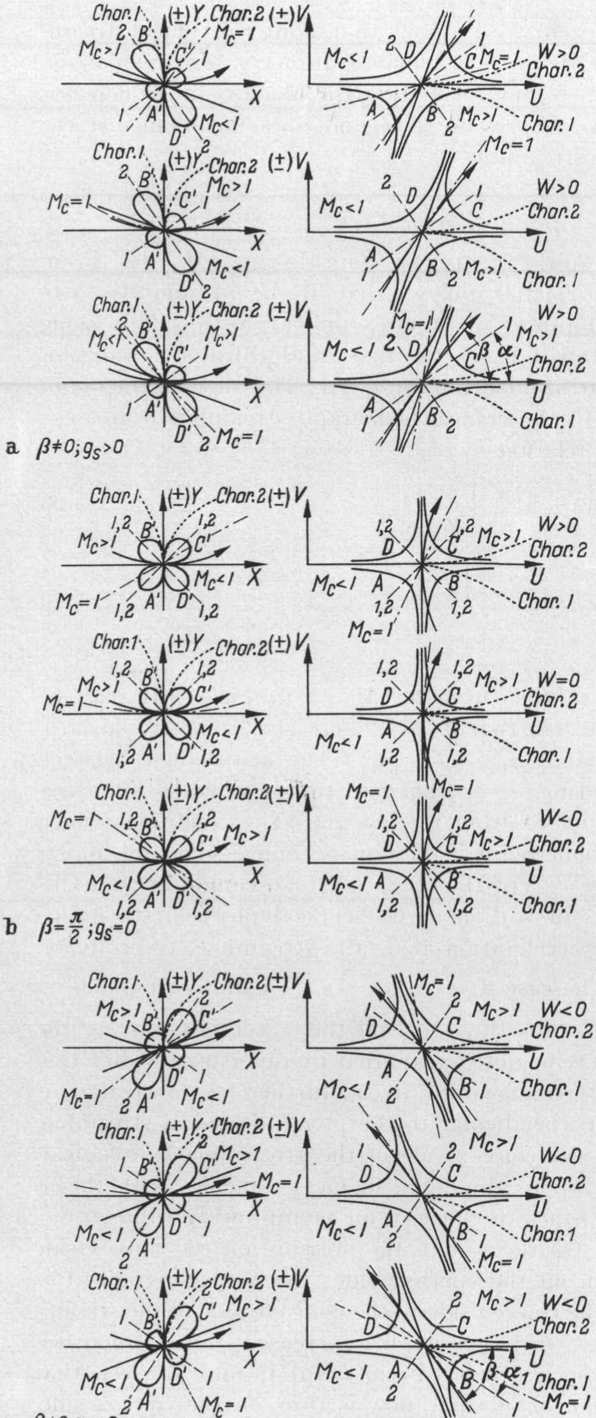

Fig. 4a—c. Typical conditions at a hyperbolic point of a conical-sonic line

concave side of the streamline and the negative U direction to the Y direction on the convex side.

It follows from (44) that the direction of the conical-sonic line is given by

$$\left(\frac{dV}{dU}\right)_{M_c=1} = -\frac{\gamma+1}{2}\,\frac{1}{W W_{UV}}, \tag{70}$$

or, from equation (30), since $W_{UU}=0$, by

$$\left(\frac{dV}{dU}\right)_{M_c=1} = \pm\frac{\gamma+1}{2a\sqrt{M^2-1}}\,\frac{1}{\sqrt{-K_G}}, \tag{71}$$

where the sign is chosen equal to the product of the signs of W, $\tan\beta$ and g_s, since W_{UV} has the sign opposite to that of the product of $\tan\beta$ and g_s. It can be remarked that if g_s and $\tan\beta$ have the same signs (or the sign of $\tan\beta$ is positive when $g_s=0$), the conical physical streamline has its concave side on the positive Y axis. If g_s and $\tan\beta$ have different signs (or the sign of $\tan\beta$ is negative when $g_s=0$), the conical physical streamline has its concave side on the negative Y axis. If the concave side of the physical conical streamline is in the positive Y direction, the conical-sonic line on the hodograph surface therefore lies in the first (and third) quadrant for $W>0$ and in the second (and fourth) quadrant for $W<0$, while it is tangent to the V axis for $W=0$ (then $M=M_c=1$). If the concave side of the physical streamline is in the negative Y direction, the conical-sonic line on the hodograph surface therefore lies in the first (and third) quadrant for $W<0$ and in the second (and fourth) quadrant for $W>0$, while again it is tangent to the V axis for $W=0$ ($M_c=M=1$). In summary, the angle on the hodograph surface between the velocity vector U and the part of the conical-sonic line on it, on the concave side of the conical physical streamline, is acute for $W>0$, equal to $\pi/2$ for $W=0$ and obtuse for $W<0$.

Since at a hyperbolic point K_G and also $a\sqrt{M^2-1}$ will be finite, for all values of M, the conical-sonic line cannot be tangent to the U axis but may have any other direction. On the unit sphere the conical-sonic line therefore cannot be normal to the physical conical streamline.

Again it may be deduced from (67) that, regardless of the value of the acceleration along the streamline, M_c may increase, decrease or remain stationary along the conical streamline for a point on the conical-sonic line. This also follows from the result that the conical-sonic line may have any direction (except that normal to the conical physical streamline). The various possible directions of the conical-sonic line with respect to the conical streamline are illustrated in Fig. 4.

The variation along the conical-sonic line of U_n, the velocity component normal to the radius, is of interest because it shows a behavior different from that for two-dimensional plane flow. From equations (42a), (42b) and (70) it may be shown that for $M_c=1$,

$$\left(\frac{dU_n}{dU}\right)_{M_c=1} = \frac{1-\gamma}{2}; \tag{72}$$

thus $dU_n/dU<0$ for $\gamma=1.4$. The velocity component normal to the radius increases along the conical-sonic line on the hodograph surface in that direction which makes an obtuse angle with the velocity vector U. In order to investigate the variation of U_n along the conical-sonic line on the unit sphere, consider first the case $g_s=0$, as sketched in Fig. 4b. It may then be shown that along the conical-sonic line on the unit sphere U_n increases in the direction which makes an obtuse angle with the velocity vector U when $W>0$; that U_n increases in the direction which makes an acute angle with the velocity vector U when $W<0$; while U_n remains stationary when $W=0$. By considering the properties of the mapping when $g_s\neq 0$ (Figs. 4a and 4c), the same conclusions may be seen to hold. The first result was also given in [*17*], where it was tacitly assumed that $W>0$ ($v_r>0$ in the notation of [*17*]). For the direction along the conical-sonic line in which U_n increases, since $U_n=M_c\,a=a$, it follows that a increases; from (2) it follows that q decreases; thus W decreases, while from Bernoulli's law it follows that p increases.

The conical hodograph characteristics, as given by (20), are both tangent to the U axis. Their geodesic curvature $\varkappa_g$ may be obtained by differentiating (19) along a characteristic. By use of (35), for the image on the hodograph surface of a point $X=Y=0$ we obtain

$$\varkappa_g = \pm\frac{\gamma+1}{2a\sqrt{M_c^2-1}} + \frac{2W}{aM_c^2}\left[W_{UV} \pm \sqrt{M_c^2-1}\,W_{VV}\right], \tag{73}$$

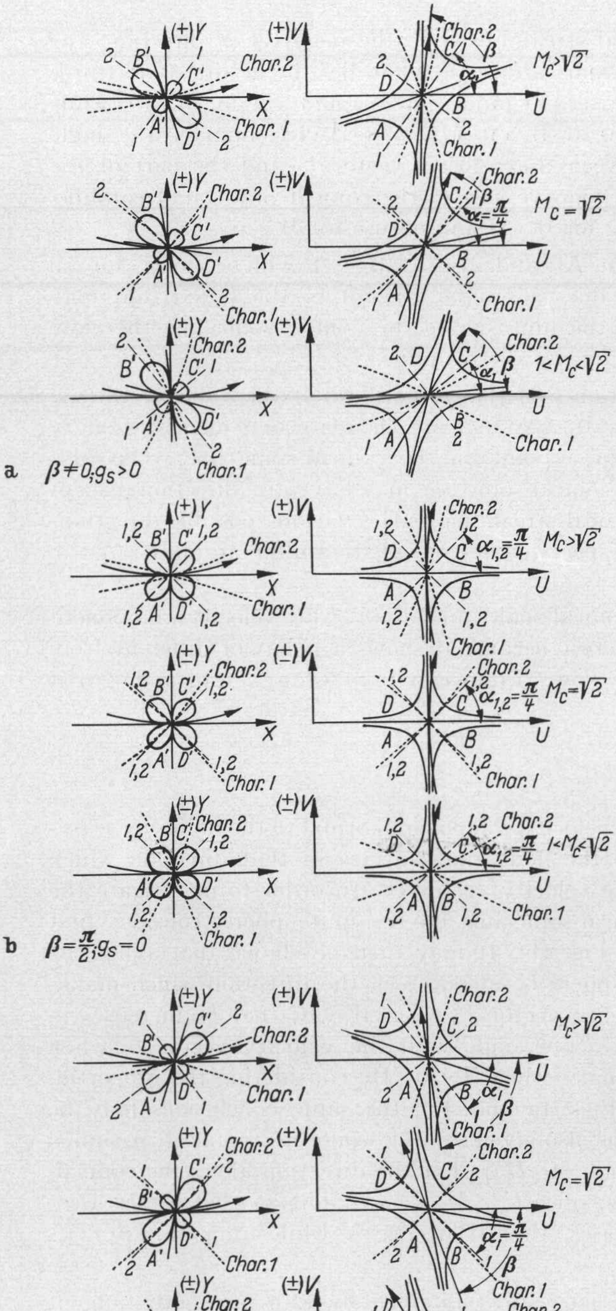

Fig. 5 a—c. Typical conditions at a hyperbolic point of a conical-supersonic flow

where the $\pm$ signs in equations (73) and (20) are associated and $\varkappa_g$ is positive if the concave side is on the positive V direction. At a conical-sonic point the curvatures of these characteristics thus approach $\pm\infty$. Both characteristics curve away from the U axis, and their images, the physical conical characteristics, both curve away from the Y axis. The physical conical characteristics lie on the concave side of the physical conical streamline, since this is the conical-supersonic region.

γ) Conical-supersonic flow

At a hyperbolic point, conical-supersonic flow can also occur. From (64) and (65) and from Fig. 2, conditions which may be encountered at such a point may be determined. The most characteristic of them are sketched in Fig. 5, and again it may be seen that reversal of the flow may be used to deduce Figs. 5a and 5c from each other. These conditions are largely similar to those at a hyperbolic point of a conical-sonic line, or a conical-subsonic flow, as discussed above. It can be remarked, however, that the conical hodograph streamline cannot lie in the region around the U axis enclosed by conical hodograph characteristics, since $|\beta| > |\arctan\sqrt{M_c^2 - 1}|$. Also it follows from equations (64) and (65) that $|\beta| \geqq |\alpha_1|$, so that the major principal axis lies between the hodograph streamline and the U

axis. The direction of the conical hodograph characteristics with respect to the direction of the major axis depends on the conical Mach number M_c. For $M_c \leqq \sqrt{2}$, it follows that $|\alpha_1| \geqq |\text{arc tan} \sqrt{M_c^2 - 1}|$, and for $M_c \geqq \sqrt{2}$, $|\alpha_1| \leqq |\text{arc tan} \sqrt{M_c^2 - 1}|$. If $M_c \to 1$, conditions at a conical-sonic line as discussed before are again found. The other limiting case occurs when $M_c \to \infty$.

Since U remains finite, $a \to 0$ when $M_c \to \infty$, and since q remains finite, $M = q/a \to \infty$. The angle of the major axis α_1 and the angle of the conical hodograph streamline β are obtained from (64) and (65):

$$\tan \alpha_1 = \pm \sqrt{-\frac{\varrho_1}{\varrho_2}}, \tag{74}$$

and

$$\tan \beta \to \pm \infty. \tag{75}$$

These relations are illustrated by the curve for $M_c \to \infty$ in Fig. 2. From equation (66) it is seen that one of the asymptotes falls along the V axis; thus $W_{VV} = 0$. The other asymptote then makes the angle $\pm\left(2|\alpha_1| - \frac{\pi}{2}\right)$ with the U axis. Since ϱ_1 and ϱ_2 remain finite and $a \to 0$, it is seen from (60) that the acceleration along the streamline is equal to zero. When $M_c \to \infty$, the acceleration normal to the streamline, according to equations (45), (62) and (65), is

$$g_n = \frac{U}{r} \sqrt{-\frac{1}{K_G}}, \tag{76}$$

and the radius of curvature of the physical streamline is

$$R = \frac{q^2}{U} r \sqrt{-K_G}. \tag{77}$$

A point in a conical-supersonic flow may also be represented by an elliptic point on the hodograph surface. Typical conditions encountered at elliptic points again may be deduced from the relations given in (64) and (65), as illustrated in Fig. 2 and sketched in Fig. 6. Again, it may be seen that Figs. 6a and 6d, and Figs. 6b and 6c, may be obtained from each other through flow reversal. If $\beta = 0$, the conical streamline remains parallel to itself when transformed and thus falls along a principal axis; thus α_1 or α_2 equals zero. According to equation (36) R_V/R_U has the value $M_c^2 - 1$, so that for $M_c < \sqrt{2}$ the major axis of DUPIN's indicatrix, which is an ellipse, falls along the U axis and the minor axis along the V axis, while for $M_c > \sqrt{2}$ the minor axis falls along the U axis and the major axis along the V axis. If $M_c = \sqrt{2}$, DUPIN's indicatrix is a circle, and the point is an umbilical point. The transformation is then conformal. In Fig. 6a the situation is sketched for accelerating flow and in Fig. 6d for decelerating flow. From equation (62) it may be concluded that for accelerating flow $\varrho_1 + \varrho_2 > 0$ and, since ϱ_1 and ϱ_2 have the same sign, $\varrho_1 > 0$ and $\varrho_2 > 0$. From the Rodrigues equations (27) it is then seen that DUPIN's indicatrix $ABCD$ when mapped onto the unit sphere is compressed in the direction of the major axis and stretched in the direction of the minor axis into the ellipse $A'B'C'D'$,

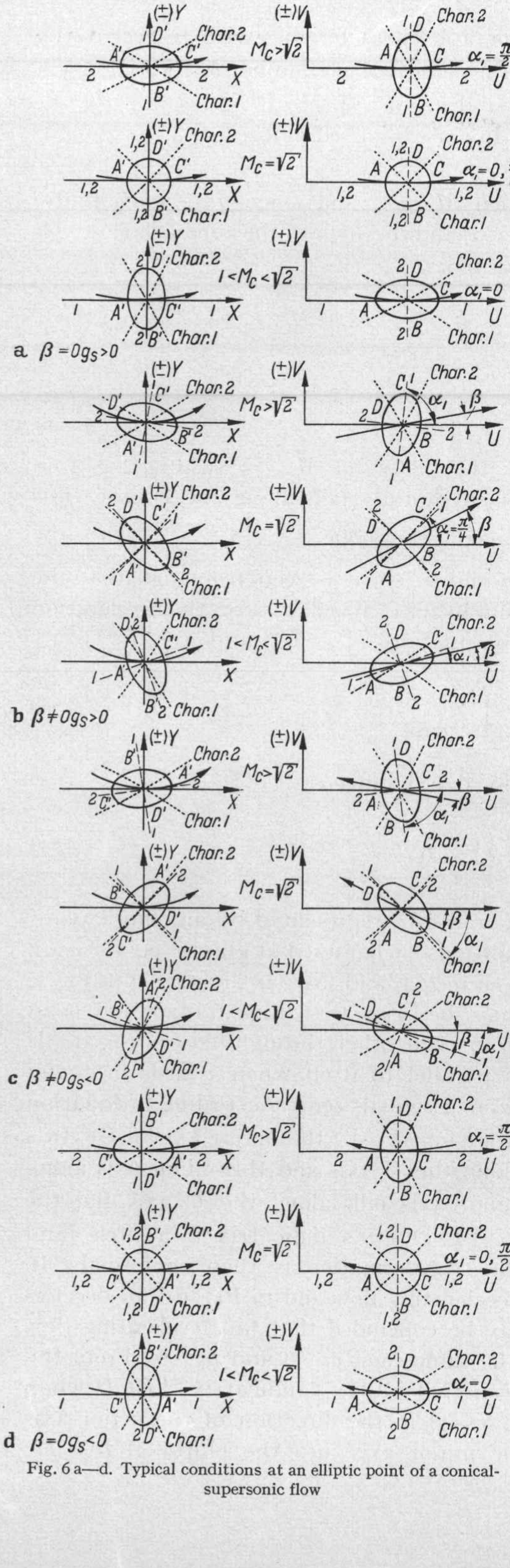

Fig. 6 a—d. Typical conditions at an elliptic point of a conical-supersonic flow

which has the same ratio of principal axes as $ABCD$. If the flow is decelerating, $\varrho_1 + \varrho_2 < 0$, and, since ϱ_1 and ϱ_2 have the same sign, it follows that $\varrho_1 < 0$ and $\varrho_2 < 0$. Dupin's indicatrix is compressed and stretched in the same manner and then rotated in its plane through 180°. Other situations that may be encountered at an elliptic point are given in the other sketches of Fig. 6. It may be noticed that the conical hodograph streamline cannot lie in the region inclosed by the conical hodograph characteristics around a line through the point considered and normal to the U axis, since $|\beta| < |\arc \tan \sqrt{M_c^2 - 1}|$ *. For finite values of M_c the acceleration along the streamline is therefore different from zero at an elliptic point, since then $|\beta| \neq \frac{\pi}{2}$. In contrast to the situation for conical-supersonic flow at a hyperbolic point, at an elliptic point $|\beta| \leqq |\alpha_1|$, while furthermore for $M_c \leqq \sqrt{2}$, $|\alpha_1| \leqq |\arc \tan \sqrt{M_c^2 - 1}|$ and for $M_c \geqq \sqrt{2}$, $|\alpha_1| \geqq |\arc \tan \sqrt{M_c^2 - 1}|$.

The case $M_c \to \infty$ does not occur at an elliptic point, since, as may be seen from equation (74), α_1 becomes imaginary for $\varrho_1/\varrho_2 > 0$.

---

* The difference between elliptic and hyperbolic points in regard to the direction of the hodograph streamline with respect to the hodograph characteristics may also be understood in the following way. The conical disturbances in the flow travel along the downstream physical characteristics which map onto those parts of the hodograph characteristics that are bisected by the U axis for an elliptic point and by a line normal to the U axis and through the point considered for a hyperbolic point. In order for these parts to be downstream characteristics the hodograph streamline should lie in the regions described.

Singular points of the transformation may now be considered as limiting cases of elliptic or hyperbolic points as $\varrho_2/\varrho_1 \to 0$. In these cases the direction of the conical hodograph streamline and the major axis approach one of the directions of the conical hodograph characteristics. Singularities thus occur for $M_c \geqq 1$. Depending on how $\varrho_1 + \varrho_2$ is chosen to vary in this limiting process, different singularities may be obtained. If $\varrho_1 + \varrho_2$ remains finite, the acceleration remains finite, $\varrho_2 \to 0$ when $\varrho_2/\varrho_1 \to 0$, while ϱ_1 remains finite. Thus the Gaussian curvature $K_G \to \pm\infty$, since $K_G = \frac{1}{\varrho_1 \varrho_2}$. A region on the unit sphere corresponds to a conical point or an edge surface, which represent a region of parallel flow or a conical simple wave flow, respectively. If $\varrho_1 + \varrho_2 \to \pm\infty$, the acceleration approaches infinity, and $\varrho_1 \to \infty$ when $\varrho_2/\varrho_1 \to 0$. Thus the Gaussian curvature K_G vanishes. The point on the hodograph surface is a parabolic point, representing a point on a limit cone or the edge point in the flow around a sharp edge.

These singularities will now be discussed in more detail in the following sections.

6. Limit cones or conical limit lines

Limit lines or surfaces probably were first discovered in some solutions of the hodograph equation for two-dimensional plane flow. A more systematic investigation of the properties of limit surfaces has since been given for two-dimensional and three-dimensional flow. For an extensive discussion, giving many references to the literature, reference may be made to [*28*].

If limit lines or surfaces appear in a solution, regions in the flow are found for which the velocity is many-valued. The transformation from the physical space into the hodograph space therefore becomes singular. Regions with a many-valued solution for the velocity are bounded by limit surfaces, so called because the direction of the flow is reversed at these surfaces and the flow thus has a limiting boundary which cannot be crossed. Two types of limit surfaces may be distinguished.

For limit surfaces of the kind most studied, the Jacobian determinant is assumed to be continuous and to vanish at this surface. In the reversal of the flow the acceleration and the pressure gradient then go to infinity. In addition, the limit surface in the physical space is the envelope of the characteristic surfaces of one family, while, correspondingly, in the hodograph space the streamlines become tangent to the characteristic surface of the other family. The other type of limit surfaces occurs when the Jacobian determinant changes sign discontinuously across a characteristic surface. The acceleration and the pressure gradient are discontinuous but remain finite, and no envelope of characteristic surfaces is formed, while accordingly the streamline in the hodograph space is not tangent to the characteristic surface.

This physically unacceptable behavior of the flow at limit surfaces can appear in the solution because it is assumed that the coefficients of viscosity and heat conduction of the gas are zero. It may then be assumed that thermodynamical processes in the gas are reversible and, if no heat is added, isentropic. In the absence of frictional forces the inertia and pressure forces controlling the motion of the gas remain in balance when the direction of the flow is reversed, so that to every isentropic solution with some prescribed stream surfaces there corresponds a solution with reversed flow. At limit surfaces, however, the reversibility of the flow occurs in such a way as to make obvious its physical impossibility, since it results in a multivalued region for the velocity. The occurence of infinite velocity gradients in the first type of limit surfaces serves as an indication that viscous stresses may no longer be neglected and that the assumption of isentropic flow, implying reversibility along the streamlines, is not justified any longer. The phenomenon of limit surfaces is analogous to ocean waves breaking on the beach, where the continued steepening of the waves is not counteracted by a mechanism analogous to the action of viscous stresses in the gas flow. In order to obtain solutions of physical value, layers called shock waves have to be introduced, these being layers in which there occur large velocity gradients and hence considerable effects of viscosity and heat conduction. If in such solutions the viscosity is assumed to approach zero, the thickness of the shock waves approaches zero, and the shock waves may be considered to be surfaces of discontinuity connecting inviscid solutions.

One is thus led to the suggestion that to every solution with a shock wave there corresponds a solution with limit surfaces along which compression occurs. If the direction of flow in these solutions is reversed, expansion occurs along the limit surfaces, and these solutions do not have physical significance, since expansion shocks cannot be formed. To every solution containing shock waves then corresponds a solution with reversed streamlines without physical meaning. It should be noted that it is not possible to state in general that to every solution with limit surfaces where compression occurs there corresponds a solution with shock waves.

Apart from the trivial case of parallel flow throughout the physical space, a stream surface in a supersonic flow may be taken to represent the surface of a body immersed in a supersonic stream, which, in general, experiences wave drag. Since wave drag is associated with the entropy rise through shock waves, shock waves occur in all flows which are supersonic in the sense taken above, and the corresponding isentropic flows contain limit surfaces. The singular behavior of the pressure waves along these surfaces appears to be an essential feature of non-linear isentropic supersonic flow.

In conical flow a limit surface is necessarily conical, so that we may speak of limit cones. The intersection of a limit cone with the unit sphere will be called a conical limit line. As will be shown now, lines of parabolic points on the hodograph surface in general represent conical limit lines of the first type, while the second type of conical limit lines may occur along a conical characteristic.

α) Conical limit lines of the first type

Consider parabolic points as limiting cases of elliptic or hyperbolic points by letting $\varrho_1 \to \infty$, thus $\varrho_2/\varrho_1 \to 0$. From equations (64) and (65) it then follows that the direction of the conical hodograph streamline and the major axis approach one of the directions of the conical characteristics. One property of a point of a limit line, namely, that the hodograph streamline is tangent to a characteristic there, is thus seen to hold also at such a parabolic point.

The two asymptotic directions coincide with the major principal direction, and DUPIN'S indicatrix consists in two parallel lines. All directions different from the major principal direction are conjugate to the latter and thus map onto the unit sphere along the direction of the minor principal axis. The hodograph characteristic which is not tangent to the major principal axis therefore also maps into this direction. In order to determine how curves on the hodograph surface which are tangent to the major principal axis are transformed, it is necessary to consider the third derivatives. Two relations between the four third derivatives at a point of the hodograph surface are given by differentiation of the differential equation (18).

By partial differentiation with respect to u and v in a co-ordinate system where the w axis is taken in the direction of the normal at the point considered (that is, the direction of the radius in the physical space), for the third derivatives at that point there follow the expressions

$$\begin{aligned}&\left(1-\frac{v^2}{a^2}\right)w_{uuu}+2\frac{u\,v}{a^2}w_{uuv}+\left(1-\frac{u^2}{a^2}\right)w_{uvv}-2\frac{u\,w}{a^2}(w_{uu}w_{vv}-w_{uv}^2)-\\&-(\gamma-1)\frac{u\,v^2}{a^4}w_{uu}+2\frac{v}{a^2}\left\{1+(\gamma-1)\frac{u^2}{a^2}\right\}w_{uv}-\frac{u}{a^2}\left\{2+(\gamma-1)\frac{u^2}{a^2}\right\}w_{vv}=0,\end{aligned}\tag{78}$$

and

$$\begin{aligned}&\left(1-\frac{v^2}{a^2}\right)w_{uuv}+2\frac{u\,v}{a^2}w_{uvv}+\left(1-\frac{u^2}{a^2}\right)w_{vvv}-2\frac{v\,w}{a^2}(w_{uu}w_{vv}-w_{uv}^2)-\\&-\frac{v}{a^2}\left\{2+(\gamma-1)\frac{v^2}{a^2}\right\}w_{uu}+2\frac{u}{a^2}\left\{1+(\gamma-1)\frac{v^2}{a^2}\right\}w_{uv}-(\gamma-1)\frac{u^2\,v}{a^4}w_{vv}=0.\end{aligned}\tag{79}$$

It appears convenient for present purposes to rotate the axes around the w axis, so that the u axis becomes parallel to the major axis and the v axis parallel to the minor axis at the point considered, and $u>0$ at this point. Then, since at a parabolic point $w_{uu}=w_{uv}=0$, $w_{vv}=-\frac{1}{\varrho_2}$, $u/a=1$ and $v/a=\mp\sqrt{M_c^2-1}$, (78) and (79) yield

$$-(M_c^2-2)\,w_{uuu}\mp 2\sqrt{M_c^2-1}\,w_{uuv}+\frac{\gamma+1}{a\,\varrho_2}=0,\tag{78a}$$

and

$$\pm(M_c^2-2)\,w_{uuv}+2\sqrt{M_c^2-1}\,w_{uvv}+\frac{\gamma-1}{a\,\varrho_2}\sqrt{M_c^2-1}=0.\tag{79a}$$

Let the co-ordinates at a point be given by $u=u_1$, $v=v_1$ and $w=w_1$. A Taylor expansion including terms up to the third order then gives at such a point

$$\begin{aligned}w=w_1&+\frac{1}{2}\left[-\frac{1}{\varrho_1}(u-u_1)^2-\frac{1}{\varrho_2}(v-v_1)^2\right]+\\&+\frac{1}{6}\left[w_{uuu}(u-u_1)^3+3\,w_{uuv}(u-u_1)^2(v-v_1)+\right.\\&\left.+3\,w_{uvv}(u-u_1)(v-v_1)^2+w_{vvv}(v-v_1)^3\right]+\cdots.\end{aligned}\tag{80}$$

Consider a curve at (u_1, v_1, w_1) making an angle α_h with the major principal axis and having a geodesic curvature $\varkappa_g$. The equation of such a curve may be written as

$$v-v_1=\tan\alpha_h(u-u_1)+\tfrac{1}{2}\varkappa_g\cos^{-3}\alpha_h(u-u_1)^2+\cdots.\tag{81}$$

If this expression is put into equation (80) after the first derivatives of w are taken, the image of this curve on the unit sphere may be seen to subtend with the major principal direction an angle α_{ph} given by

$$\tan\alpha_{ph} = \lim_{(u-u_1)\to 0} \frac{-\frac{1}{\varrho_2}\tan\alpha_h(u-u_1) + \left[-\frac{1}{2\varrho_2}\varkappa_g\cos^{-3}\alpha_h + \frac{1}{2}w_{uuv} + \tan\alpha_h\, w_{uvv} + \frac{1}{2}\tan^2\alpha_h\, w_{vvv}\right](u-u_1)^2 + \cdots}{-\frac{1}{\varrho_1}(u-u_1) + \left[\frac{1}{2}w_{uuu} + \tan\alpha_h\, w_{uuv} + \frac{1}{2}\tan^2\alpha_h\, w_{uvv}\right](u-u_1)^2 + \cdots}. \tag{82}$$

If ϱ_1 and ϱ_2 are both finite and different from zero, *i.e.*, at elliptic and hyperbolic points, (28) is found again when the limit is performed. At a parabolic point $\varrho_1 \to \infty$; thus when $\alpha_h \neq 0$, equation (82) shows that all directions different from the major principal direction map into the direction of the minor principal axis, as we have noticed above. When $\alpha_h = 0$, that is, when a curve on the hodograph surface is tangent to the major axis, (82) yields

$$\tan\alpha_{ph} = \frac{-\frac{\varkappa_g}{\varrho_2} + w_{uuv}}{w_{uuu}}. \tag{83}$$

From equations (73), (45) and $\tan\beta = \pm\sqrt{M_c^2 - 1}$, the geodesic curvature of the hodograph characteristics in a parabolic point is found to be

$$(\varkappa_g)_{\text{char.}} = \pm \frac{\gamma+1}{2a\sqrt{M_c^2-1}}, \tag{84}$$

which is equal to the expression for two-dimensional plane flow if M_c is replaced by M.

By use of this result and (78a) in (83) the direction of the image of the hodograph characteristic tangent to the major principal axis is found to be

$$\tan\alpha_{ph} = \mp \frac{M_c^2 - 2}{2\sqrt{M_c^2-1}}, \tag{85}$$

which when compared with equation (10) is seen to be the direction of the corresponding conical physical characteristic. The hodograph characteristics thus map onto the physical characteristics.

It may also be seen that the conical hodograph streamline maps onto the conical physical streamline. By differentiation of (50) along the streamline it follows in the above-mentioned co-ordinate system that

$$\left(\frac{d^2 v}{du^2}\right)_s = -\varrho_2\left[\frac{v}{u}w_{uuu} + \left(2\frac{\varrho_2}{\varrho_1}\frac{v}{u} - 1\right)w_{uuv} + \left(-2\frac{\varrho_2}{\varrho_1}\frac{v}{u} + \frac{\varrho_2^2}{\varrho_1^2}\frac{v^3}{u^3}\right)w_{uvv} - \frac{\varrho_2^2}{\varrho_1^2}\frac{v^2}{u^2}w_{vvv}\right] - \frac{v}{u^2}\frac{\varrho_2}{\varrho_1}\left(1 - \frac{\varrho_2}{\varrho_1}\right), \tag{86}$$

from which the geodesic curvature of a hodograph streamline in a parabolic point may be obtained:

$$(\varkappa_g)_s = \varrho_2\left(\pm\sqrt{M_c^2-1}\,w_{uuu} + w_{uuv}\right). \tag{87}$$

Using this expression in (83) yields the correct value $(\tan \alpha_{ph})_s = \mp \sqrt{M_c^2 - 1}$. If $w_{uuu} \neq 0$, the return of a conical physical streamline at an image point of a parabolic point may be deduced. In this case, since at a parabolic point the conical hodograph streamline is in the direction of the u axis and $w_{uu} = 0$, the projection of the hodograph streamline on a normal plane through the major principal direction has a point of inflection. Since furthermore $(\tau_g)_s = 0$, the normal to the hodograph surface along a streamline thus has an extreme value at the parabolic point, and the conical physical streamline returns and exhibits a cusp. The velocity at a parabolic point changes sign, so that downstream of the parabolic point the solution on the surface $w(u, v)$ continues on the surface $-w(-u, -v)$. The rays in the physical space upstream and downstream of a line of parabolic points cover the same region, so a many-valued region on the unit sphere appears, bounded by the image points of the parabolic points. This may also be seen by noting that differentiation of (30) along a streamline at a parabolic point yields

$$\left(\frac{dK_G}{du}\right)_{s,\,K_G=0} = -\frac{w_{uuu}}{\varrho_2}, \tag{88}$$

which is different from zero if $w_{uuu} \neq 0$. A parabolic line then separates a region of elliptic points from a region of hyperbolic points. A closed curve on the hodograph surface which does not intersect itself and which is divided into two parts by a parabolic line is traversed along its image on the unit sphere in the same direction as on the hodograph surface in the region of elliptic points, but in the opposite direction in the region of hyperbolic points. A doubly covered region on the unit sphere thus exists. All curves tangent to a major principal axis, including one of the two families of characteristics and the streamlines, when mapped onto the unit sphere return and show a cusp at the image of the parabolic line. All curves which are not tangent to a major principal axis, including the other family of characteristics, are tangent to this image line. The image line is the envelope of these curves and thus also, for example is the envelope of the lines of constant speed and of one family of physical conical characteristics. The latter may also be seen by transforming the physical conical characteristics, as given by (8), to the hodograph surface by means of equation (15). The equation which follows may be written at the point considered in the form

$$K_G\left[\left(\frac{dV}{dU}\right)^2 - (M_c^2 - 1)\right] = 0. \tag{89}$$

The conical hodograph characteristics are therefore the representation of the conical physical characteristics, as might be seen by equating to zero the expression in brackets in (89) and then comparing the results with (20). Further, (89) may be satisfied along a line on the hodograph surface where $K_G = 0$. This parabolic line, when mapped to the unit sphere, will have at any point a slope equal to that of one family of physical conical characteristics. Since this line does not coincide with a characteristic, it will be the envelope of the physical characteristics of one family.

By differentiating equation (30), we may find the slope of the parabolic line, and

$$\tan \delta = \left(\frac{dv}{du}\right)_{K_G=0} = -\frac{w_{uuu}}{w_{uuv}}, \tag{90}$$

so that for $w_{uuu} \neq 0$ and w_{uuv} finite the parabolic line does not touch a major principal axis at any point.

As has been remarked previously, by equations (60), (61) and (62) the acceleration and pressure gradient go to infinity, since $\varrho_1 \to \infty$. In addition it is concluded from (63) that the radius of curvature of the spatial streamline goes to zero.

It is thus shown that the flow at a parabolic point, if $w_{uuu} \neq 0$, shows the typical behavior exhibited at limit surfaces of the first type, and that parabolic lines are the images of limit cones or conical limit lines.

The variation of M_c along the streamline at a parabolic point is related to the sign of the acceleration. From (67) it follows that for $K_G = 0$

$$\left(\frac{dM_c}{dU}\right)_s = \frac{1}{a}\left\{1 + \frac{\gamma-1}{2} M_c^2\right\}. \tag{91}$$

Since this quantity is positive, M_c increases in an accelerating flow ($g_s > 0$) and decreases in a decelerating flow ($g_s < 0$). This is at variance with the situation at elliptic and hyperbolic points, where the increase or decrease of M_c along the streamline is not determined by the sign of the acceleration alone. On the contrary, as with the geodesic curvature of the characteristics, equation (84), the local flatness of the hodograph surface ($K_G = 0$) is again expressed, since if M_c replaced by M, the same expression for the variation of M is found as in two-dimensional plane flow.

Conditions which may be encountered at a parabolic point when $w_{uuu} \neq 0$ are sketched in Fig. 7*. Again Fig. 7d may be obtained from Fig. 7a and Fig. 7c from Fig. 7b by flow reversal. Further it is seen that in an expanding flow the conical limit line is inclined along the upstream conical physical characteristic on the concave side of the streamline or along the downstream conical physical characteristic on the convex side of the streamline. If the flow is compressing, the conical limit line is inclined along the downstream conical physical characteristic on the concave side of the streamline or along the upstream conical physical characteristic on the convex side of the streamline.

If $\beta = 0$, as for example in axially symmetric conical flow, it follows at once that $M_c = 1$. From (78a) and (79a) it follows that then $w_{uuu} = -\frac{\gamma+1}{a\,\varrho_2}$ and $w_{uuv} = 0$. From (88) it is seen that

$$\left(\frac{dK_G}{du}\right)_{s,\,K_G=0,\,M_c=1} = \frac{\gamma+1}{a\,\varrho_2^2}, \tag{92}$$

so that the hyperbolic points are on the side of the origin ($U = V = 0$) with respect to the parabolic point, and the elliptic points are on the other side. For accelerating motion the flow changes from conical-subsonic to conical-supersonic flow, whereas for decelerating motion the flow is from conical-supersonic flow to conical-subsonic flow. From equation (90) it is seen that the parabolic line is perpendicular to the streamline ($\delta = \frac{1}{2}\pi$), as is the conical-sonic line, as may be concluded from (44). On the unit sphere the conical limit line is also perpendicular to the streamline. If the flow is axially symmetric,

* The co-ordinate axes X, Y and Z, and U, V and W are defined by the velocity components on the upstream side of the parabolic point.

the two lines coincide, so that each conical limit line in an axi-symmetric conical flow, which is represented by a parabolic line on the hodograph surface, is a conical-sonic limit line.

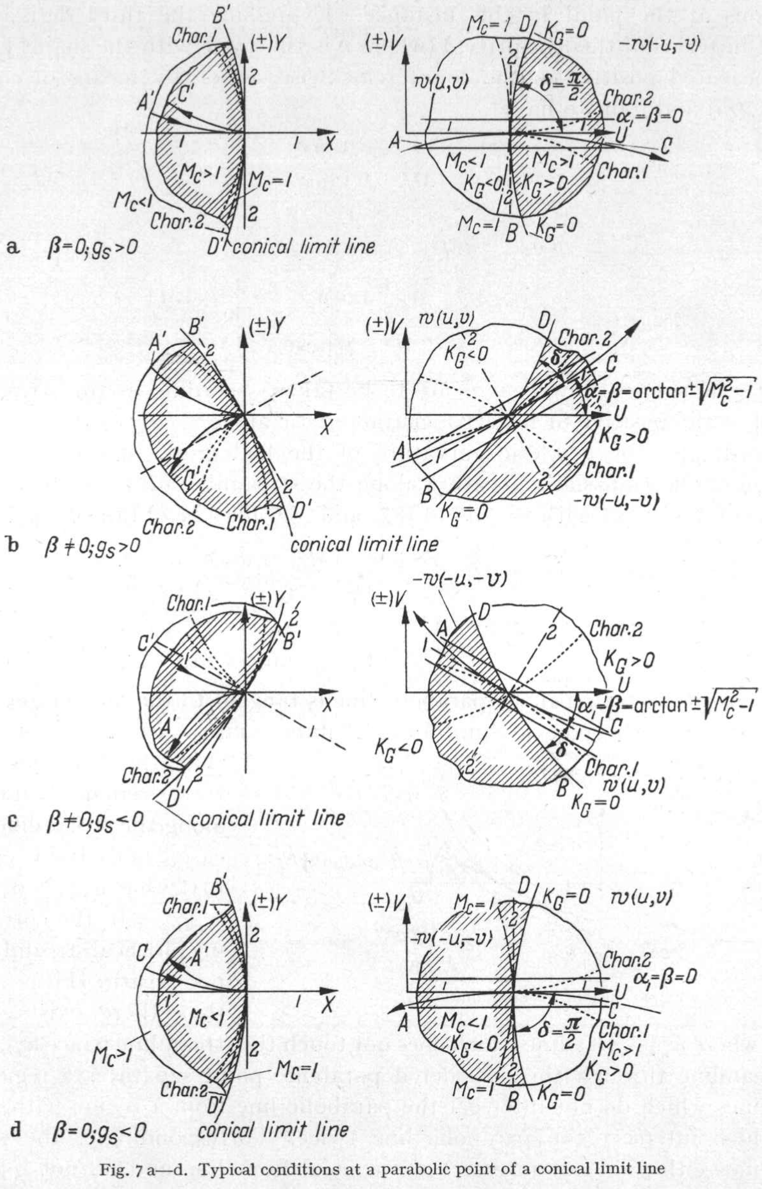

Fig. 7 a—d. Typical conditions at a parabolic point of a conical limit line

Singularities on conical limit lines may now be investigated by considering third and higher derivatives at parabolic points. It may be expected that because of the planar character of the hodograph surface at parabolic points these singularities will bear a marked resemblance to those of limit lines in two-dimensional plane flow.

For example, if the third derivatives are taken into account, just as in two-dimensional plane flow cusps of a conical limit line may be encountered. The slope of the parabolic line may be taken as the parameter which governs conditions at the point in this instance. Expressing the third derivatives of interest in terms of this quantity δ (where δ is the angle with the major principal axis, measured positive in the counterclockwise sense), by means of equations (78a), (79a) and (90) we have

$$w_{uuu} = -\frac{\gamma+1}{a\,\varrho_2}\,\frac{\tan\delta}{-(M_c^2-2)\tan\delta \pm 2\sqrt{M_c^2-1}}, \tag{93}$$

$$w_{uuv} = \frac{\gamma+1}{a\,\varrho_2}\,\frac{1}{-(M_c^2-2)\tan\delta \pm 2\sqrt{M_c^2-1}}, \tag{94}$$

$$w_{uvv} = \frac{\gamma-1}{a\,\varrho_2}\,\frac{(M_c^2-2)\left(\frac{1}{2}\tan\delta \mp \frac{\gamma-1}{\gamma+1}\right) \mp \sqrt{M_c^2-1}}{-(M_c^2-2)\tan\delta \pm 2\sqrt{M_c^2-1}}, \tag{95}$$

where the upper and lower signs are to be taken according as the streamline is inclined at the positive or negative characteristic angle.

Accordingly, the geodesic curvature of the hodograph streamline and the variation of the Gaussian curvature along the streamline may also be expressed in terms of δ, so that with the aid of (87) and (88) may be obtained the formulae

$$(\varkappa_g)_s = \frac{\gamma+1}{a}\,\frac{\mp\sqrt{M_c^2-1}\tan\delta + 1}{-(M_c^2-2)\tan\delta \pm 2\sqrt{M_c^2-1}}, \tag{96}$$

$$\left(\frac{dK_G}{du}\right)_{K_G=0,\,s} = \frac{\gamma+1}{a\,\varrho_2^2}\,\frac{\tan\delta}{-(M_c^2-2)\tan\delta \pm 2\sqrt{M_c^2-1}}. \tag{97}$$

It may now be seen that if the parabolic line is tangent to the hodograph streamline, when $\delta=0$ the conical limit line exhibits a cusp. From (97) it appears that the Gaussian curvature remains stationary along the streamline in this case, and from equation (93), that $w_{uuu}=0$. If then $w_{uuuu} \neq 0$, the corresponding physical streamline does not return. If it is assumed that there exists on the surface where $w_{uuu}=0$ a line which does not touch the streamline (since $w_{uuuu} \neq 0$), the streamline through the considered parabolic point separates a region with streamlines which do not intersect the parabolic line from a region with streamlines which intersect the parabolic line twice. Correspondingly, the physical streamlines either do not intersect the conical limit line and do not return, or reverse twice, at the first and second branches of the limit line successively. A sketch of the conditions at a cusp of the limit line is given in Fig. 8. In order for the characteristics to map in the way indicated in this figure, it may be noted that the hodograph streamline should osculate the hodograph characteristic. From (84) and (96) it may be shown that for $\delta=0$ the geodesic curvature of the streamline and its tangent characteristic are equal.

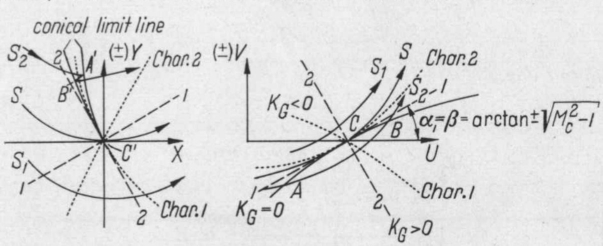

Fig. 8. Cusp at a conical limit line

For given values of γ, a, M_c and ϱ_2, the quantity δ uniquely determines the third derivatives w_{uuu}, w_{uuv} and w_{uvv}, unless the determinant of the system of equations (78a), (79a) and (90) vanishes. This determinant is equal to

$$\mp 2\sqrt{M_c^2-1}\,[-(M_c^2-2)\tan\delta \pm 2\sqrt{M_c^2-1}];$$

thus it is equal to zero for $M_c=1$ and for $\tan\delta = \pm 2\sqrt{M_c^2-1}\,[M_c^2-2]^{-1}$. The case $M_c=1$ was discussed above, where it was shown that $\delta=\frac{\pi}{2}$, $w_{uuu}=-\frac{\gamma+1}{a\,\varrho_2}$ and $w_{uuv}=0$. In the latter case the parabolic line is tangent to the other hodograph characteristic, and the system becomes dependent if $\varrho_2\to\infty$. In accordance with the theory of characteristics, it is possible to assign not only δ and w_{vvv} but also one of the other third derivatives.

Among the singularities of higher order, the parabolic line that coincides entirely with a streamline is of particular interest. This line is a plane curve which coincides with a conical characteristic. At all points of it the normal to the hodograph surface is also the binormal to the plane curve, so that one point on the unit sphere corresponds to a curve on the hodograph surface. Since $\varrho_1\to\infty$, the accelerations along and normal to the streamline are infinite, as may be deduced from (60) and (62), while the radius of curvature of the physical streamline is zero. The flow is one around a sharp edge, and conditions at the edge point are given by the parabolic line on the hodograph surface. Such a singularity may be met for example in the flow around a subsonic leading edge of a flat delta wing at incidence or in the flow around the tip of a flat rectangular wing at an angle of attack with respect to a parallel supersonic flow. This type of singularity is different from the actual conical limit lines, since no flow reversal occurs, but is mentioned here because, as in the case of conical limit lines, the Jacobian of the transformation vanishes.

β) Conical limit lines of the second type

In order to recognize the occurence of conical limit lines of the second type we now consider how the conical hodograph characteristics determine the geometry of an integral surface in the hodograph space.

Let a region R of an integral surface be given, including the boundary C; we ask how this surface can be extended into a region S, adjacent to R along C, in such a way that $w(u,v)$, $w_u(u,v)$ and $w_v(u,v)$ are continuous across C. In the region S the co-ordinates of the points and the tangent planes to the surface along C are thus known. Furthermore, the shape of C, being the boundary of the region R, is known, and since C is also a curve in S, the geodesic torsion and the normal curvature of C, being the two geometric properties determined by the second derivatives in S, are known. In addition, S is known to satisfy the differential equation (18). Written in the U, V and W co-ordinate system, the following equations are thus obtained:

$$W_{UU}+(1-M_c^2)\,W_{VV}=0, \tag{98}$$

$$-\sin\alpha\cos\alpha\,W_{UU}+(\cos^2\alpha-\sin^2\alpha)\,W_{UV}+\sin\alpha\cos\alpha\,W_{VV}=\tau_g, \tag{99}$$

$$\cos^2\alpha\,W_{UU}+2\sin\alpha\cos\alpha\,W_{UV}+\sin^2\alpha\,W_{VV}=-\varkappa_n, \tag{100}$$

where τ_g and $\varkappa_n$ are the geodesic torsion and the normal curvature of the curve C on the surface, respectively, making an angle α (α measured positive in the counterclockwise direction) with the U axis.

Two cases may now occur; either the rank of the coefficient matrix is equal to 2 or equal to 3, while the rank cannot be equal to 1. In the first case equations (98)—(100) may be solved for the second derivatives in S to obtain the same values as those on C in R. Secondly, if $\alpha = \operatorname{arc}\tan \pm\sqrt{M_c^2 - 1}$, the rank is 2, and the equations are dependent if there is a linear dependency between τ_g and $\varkappa_n$. In this case one of the second derivatives in S may be chosen, so that a jump in the curvature occurs along C, which is then a characteristic.

For the geodesic torsion of a characteristic then follows the formula

$$(\tau_g)_{\text{char.}} = \frac{2 - M_c^2}{M_c^2}\left[W_{UV} \pm \sqrt{M_c^2 - 1}\, W_{VV}\right], \tag{101}$$

and for the normal curvature of the characteristic,

$$(\varkappa_n)_{\text{char.}} = \mp \frac{2\sqrt{M_c^2 - 1}}{M_c^2}\left[W_{UV} \pm \sqrt{M_c^2 - 1}\, W_{VV}\right], \tag{102}$$

where upper and lower signs in equations (101), (102) and (20) correspond.

From this dependence of $(\tau_g)_{\text{char.}}$ and $(\varkappa_n)_{\text{char.}}$ it follows that

$$(\tau_g)_{\text{char.}} = \pm \frac{M_c^2 - 2}{2\sqrt{M_c^2 - 1}}\, (\varkappa_n)_{\text{char.}}. \tag{103}$$

Geometrically, this result may be understood by noting that the conical characteristics form a conjugate net on the hodograph surface. If one travels along one characteristic, the tangent plane thus rotates around the other characteristic direction. The geodesic torsion of the conical characteristic is therefore determined by its shape and by the normal to the surface at the point considered, since these fix the conical Mach number M_c and $(\varkappa_n)_{\text{char.}}$.

Also, the geodesic curvature of the characteristic may be expressed in this way by means of (73) and (102):

$$(\varkappa_g)_{\text{char.}} = \pm \frac{\gamma + 1}{2a\sqrt{M_c^2 - 1}} \mp \frac{W}{a}\, \frac{1}{\sqrt{M_c^2 - 1}}\, (\varkappa_n)_{\text{char.}}. \tag{104}$$

If a jump in W_{VV} across C is indicated by $\{W_{VV}\}$, where $\{W_{VV}\} = (W_{VV})_S - (W_{VV})_R$ (the indices S and R refer to conditions on C in S and R, respectively), the discontinuities in W_{UV} and W_{VV} are obtained from (98) and (101), as follows:

$$\begin{aligned} \{W_{UU}\} &= (M_c^2 - 1)\,\{W_{VV}\}, \\ \{W_{UV}\} &= \mp \sqrt{M_c^2 - 1}\,\{W_{VV}\}, \\ \{W_{VV}\} &= \{W_{VV}\}. \end{aligned} \tag{105}$$

From these results the discontinuity across C of the Gaussian curvature may be calculated, and it is found that

$$\{K_G\} = \pm 2\sqrt{M_c^2 - 1}\left[W_{UV} \pm \sqrt{M_c^2 - 1}\, W_{VV}\right]\{W_{VV}\},$$

or

$$\{K_G\} = -M_c^2 (\varkappa_n)_{\text{char.}}\, \{W_{VV}\}. \tag{106}$$

By differentiation of the differential equation (18) on both sides of C, the jump across C may be seen to obey along C a differential equation governing the propagation of the jump disturbance along this characteristic. If, then, somewhere on C a discontinuity $\{K_G\}$ is introduced which propagates along C in such a way that a part of C exists where the Gaussian curvature changes sign across C, this part is a curve on the surface separating a region of elliptic points from a region of hyperbolic points. There is then a doubly covered region on the unit sphere, bounded by the physical conical characteristic C', which is the image of C. The acceleration has a discontinuity across C but remains finite as long as the principal radii of curvature remain finite. Accordingly, the physical streamline returns and has a discontinuity in curvature at the characteristic C' where it has a cusp. The conical hodograph streamlines and the lines of curvature on the hodograph surface have corners at C.

It might possibly be conjectured that the different nature of the two types of limit lines corresponds to whether they lie in or on the boundary of an independent hyperbolic region (second type of limit line) or a hyperbolic region depending on an elliptic region (first type of limit line).

7. Conical simple wave flow

Spatial simple wave flows may be defined as flows where the velocity vector and the state of the gas do not vary in planes tangent to the characteristic surfaces originating at points of these planes. If all these planes go through at least one common point, the flow is conical, and the point of intersection is the center of the conical field*. The intersections with the unit sphere are great circles which are conical characteristics, since each plane is the envelope of characteristic surfaces originating on rays in it. The name "simple waves" refers to the fact that the conical characteristics of the other family do not carry flow disturbances, because the state of motion of the gas remains constant when crossing these conical characteristics along a straight characteristic of the first family.

In order to investigate the behavior of conical simple wave flow in the hodograph space, consider first an integral surface R with boundary B. Let this surface be divided into three regions R_1, S and R_2 by the characteristics C_1 and C_2 in a manner as sketched in Fig. 9. The image of R on the unit sphere is called R', while all curves and points on R' corresponding to their images on R are denoted by primes. In order to correspond to physical reality, as given by the underlying assumptions of isentropic flow throughout the region bounded by B', it may be assumed that $w(u, v)$, $w_u(u, v)$ and $w_v(u, v)$ are continuous functions on R. The region S may consist of elliptic, parabolic and hyperbolic points, and characteristics along which discontinuities in the second or higher derivatives occur. It is thus assumed that the Gaussian curvature remains finite in S. Chose a point P on C_1, let the conical hodograph characteristic of the other family through P be $\overline{C}_1$ and the streamline s. Construct

* Spatial simple wave flows which are not conical are excluded from the present discussion. An example of such a flow is the isentropic supersonic flow over a curved two-dimensional profile in a homogeneous stream.

a plane N at P normal to C_1 and at P' a plane N' parallel to N. Since the normal at P lies in N, O' lies in N', and N' cuts the unit sphere along a great circle, which is denoted by $P'Q'$, while its image on R is denoted by PQ. The image of $\bar{C}_1$ on the unit sphere is $\bar{C}_1'$, and since at P' the line $P'Q'$ is normal to C_1, $\bar{C}_1'$ is tangent to $P'Q'$ at P'. Call U the intersection of $\bar{C}_1$ and C_2, and call its image U'. The region S' may now be considered to become a simple wave region if discontinuities in the Gaussian curvature are introduced along C_1 and C_2 and if R_2 and S are deformed in such a way that U' approaches Q', while $\bar{C}_1'$ coincides with $P'Q'$ if the radius of curvature of the arc PQ approaches zero when Q coincides with P, wherever the point P is chosen on C_1. In this process the normals to the surface along C_2 are chosen to vary in such a way

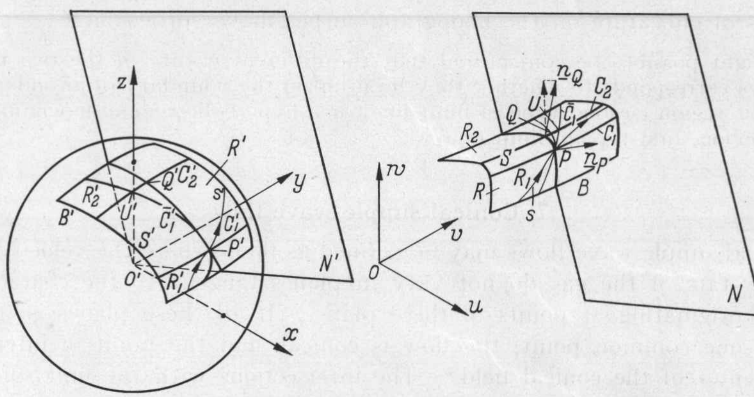

Fig. 9. Conical simple wave flow

that they do not coincide with the normals along C_1 when C_1 and C_2 have come together. According to the definition of a conical simple wave flow given above, in this way S' becomes a region with straight characteristics along which the velocity vector and the state of the gas are constant. In the hodograph space the simple wave flow is then given by a surface S of zero breadth, bounded along its length by two conical characteristics C_1 and C_2 and in general imbedded between the regions R_1 and R_2. Such a surface will be called an edge surface. It follows from EULER'S theorem, equation (24), that if the radius of curvature in any direction approaches zero, one of the principal radii of curvature must approach zero. On the edge surface S, therefore, $\varrho_2 \to 0$, and the Gaussian curvature goes to infinity. DUPIN'S indicatrix of points on S degenerates into two isolated points with co-ordinates $\pm\sqrt{|\varrho_1|}$ on the major principal axis and the point midway between of them, representing $\sqrt{|R|}=0$. Points on the edge surface may be distinguished by their normals, and from the limiting process it follows that at all points having the same velocity vector q the normals lie in a plane normal to C_1 (or C_2)*. On S, the images of different physical streamlines in S' flow together over the same space curve C_1 (or C_2); they have corners where they leave or enter S from R_1 or R_2. As has been noted in the previous

* It may be clear by now that it is not an arbitrary curve on R that may be chosen as a sharp edge in the hodograph surface, where w_u and w_v are discontinuous.

discussion of the transformation for finite values of the Gaussian curvature, when $\varrho_2/\varrho_1 \to 0$, the major principal axis falls along the direction of one of the conical characteristics, which then also is the direction of the conical streamline. From (32) it may be seen that when $\varrho_2 = 0$, if two directions are conjugate, at least one of them coincides with the major principal direction, so all directions are conjugate to the major principal axis. Thus all lines having such a direction, including the conical hodograph characteristic which is not tangent to the major principal axis and the line of constant speed, map on the unit sphere into the direction of the minor principal axis, which then also is the direction of the straight conical characteristic. In order to determine the transformation of a curve tangent to the major principal direction the derivation of equation (28) may be repeated in a more general form. Using (15) then yields the relation

$$\tan \alpha_{ph} = \frac{w_{uv} + w_{vv} \tan \alpha_h}{w_{uu} + w_{uv} \tan \alpha_h}, \tag{107}$$

where the w axis again is chosen parallel to the normal to the surface, but the u and v axes are still arbitrary. If they are chosen parallel to the principal axes, (28) is found again. If the u axis is chosen in the direction of particular interest, $\tan \alpha_h \equiv 0$, and equation (107) together with (25) and (26) yield the expression

$$\tan \alpha_{ph} = -\frac{\tau_g}{\varkappa_n}. \tag{108}$$

Therefore, since the geodesic torsion of the lines of curvature is zero, the direction of a tangent to these lines transforms parallel to itself.

The direction of the image of the characteristic tangent to the major principal axis can be obtained by the aid of (103) and (108):

$$\tan \alpha_{ph} = \mp \frac{M_c^2 - 2}{2\sqrt{M_c^2 - 1}}, \tag{109}$$

so again we see that the hodograph characteristics map onto the physical characteristics.

In order to investigate the transformation of the streamline its geodesic torsion has to be determined. By repeated use of equations (25) and (26) along the principal directions, the second derivatives may be expressed as a function of ϱ_1, ϱ_2 and α_1. With these results and equations (64) and (65) the geodesic torsion of the hodograph streamline may be obtained from (26) as

$$(\tau_g)_s = \pm \frac{1}{\varrho_1} \frac{\sqrt{\left\{1 - \frac{\varrho_2}{\varrho_1}(M_c^2 - 1)\right\}\left\{M_c^2 - 1 - \frac{\varrho_2}{\varrho_1}\right\}}}{\left(1 + \frac{\varrho_2}{\varrho_1}\right)^2 - \frac{\varrho_2}{\varrho_1} M_c^2}, \tag{110}$$

so that, when $\varrho_2 = 0$, it follows that

$$(\tau_g)_s = \pm \frac{1}{\varrho_1} \sqrt{M_c^2 - 1}. \tag{111}$$

If this value is used in equation (108), and if further it is noticed that for $\varrho_2=0$, $(\varkappa_n)_s=\frac{1}{\varrho_1}$, the direction of the image on the unit sphere of the hodograph streamline turns out to satisfy

$$\tan\alpha_{ph}=\mp\sqrt{M_c^2-1}, \tag{112}$$

which is equal to the expression for the conical physical streamline. The conical streamlines on the unit sphere and on the edge surface thus map onto each other.

In order to carry over the reasoning for points on the surface with finite Gaussian curvature to points on the edge surface these points may be distinguished in a similar fashion as elliptic, parabolic and hyperbolic points. It should be noted that then the edge surface coincides with a space curve. Taking the tangent, principal normal and the binormal of this space curve as a reference system, the normals to the edge surface at points with the same radius vector q are seen to lie in the normal plane of the space curve. They can be given by the angle ϑ with the binormal at the corresponding point of the space curve, where ϑ may be chosen as measured from the direction of the binormal, increasing when turning to the principal normal over the shortest angle. According to MEUSNIER'S theorem, a curve on the edge surface in the major principal direction has geodesic curvature and normal curvature given by

$$\varkappa_g=\frac{1}{\varrho}\cos\vartheta, \tag{113}$$

and

$$\varkappa_n=-\frac{1}{\varrho}\sin\vartheta, \tag{114}$$

where ϱ is the radius of curvature of the space curve. Since this curve also is a characteristic, application of (113) and (114) for $\vartheta=\frac{1}{2}\pi$ and use of (104) gives

$$\varrho=-\frac{2}{\gamma+1}\,q_n, \tag{115}$$

where q_n is the component of q along the principal normal ($q_n\leqq 0$ since $\varrho\geqq 0$).

For the major principal radius of curvature of a point on the edge surface it follows from equations (114) and (115) that

$$\varrho_1=-\frac{2}{\gamma+1}\,\frac{q_n}{\sin\vartheta}. \tag{116}$$

If now a closed curve on the edge surface is traversed, the end points of the unit normal vectors to the surface describe a curve which is traversed in the same direction as its image curve on the unit sphere if $\varrho_1>0$ and in the opposite direction if $\varrho_1<0$ in the enclosed region. Accordingly, points on this surface will be called elliptic edge points if $\varrho_1>0$ or hyperbolic edge points if $\varrho_1<0$. If $\varrho_1\to\infty$, the point will be called a parabolic edge point. From (116) it follows that points for which $\pi<\vartheta<2\pi$ are elliptic edge points, and those for which $0<\vartheta<\pi$ are hyperbolic edge points, while for parabolic edge points $\vartheta=0$ or π. It may be superfluous to remark that the edge surface does not necessarily extend over the entire range of ϑ.

The acceleration along the streamline follows from equations (60) and (116):

$$g_s = -\frac{2}{\gamma+1}\frac{a^2}{r}\frac{q_n}{q\sin\vartheta}, \tag{117}$$

so that at elliptic edge points the flow is accelerating, and at hyperbolic edge points the flow is decelerating. As may easily be seen from the transformation, in an accelerating conical simple wave flow the straight conical physical characteristics are inclined in the upstream direction on the concave side of the streamline and in the downstream direction on the convex side of the streamline, while for a decelerating flow the straight conical characteristics are inclined downstream on the concave side of the streamline or upstream on the convex side of the streamline.

The transformation from the unit sphere to the edge surface exhibits a singularity at a parabolic edge point. Two lines of parabolic edge points ($\vartheta=0$ and $\vartheta=\pi$) may exist on the edge surface, separating a region of elliptic edge points from a region of hyperbolic edge points. The geodesic torsion of a line of parabolic edge points is by definition equal to the torsion of the space curve which coincides with the edge surface.

Consider first the case when τ, the torsion of the space curve, is not equal to zero. Since $\varrho_1\to\infty$ at a parabolic edge point, it follows from equations (111) and (103) that the geodesic torsions of the hodograph streamline and of the characteristic in the streamline direction are zero. When crossing the line of parabolic edge points these curves thus enter a region with a different sign of ϱ_1 and therefore go in either direction from a region of elliptic edge points to a region of hyperbolic edge points. A doubly covered region on the unit sphere appears, and, since $(\tau_g)_s=(\tau_g)_{\text{char.}}=0$, the physical streamlines and the family of curved physical characteristics return at the image of the line of parabolic edge points. According to (108), since $\tau_g=\tau\neq 0$ and $\varkappa_n=0$, this image line is everywhere tangent to the direction of the minor principal axis. According to (28) a characteristic of the family of straight physical characteristics is also tangent to this direction. Since the parabolic edge line does not coincide with such a characteristic, the image line is the envelope of the family of straight physical characteristics. As can easily be seen, the curved characteristics cannot form an envelope. The reversal of the streamline is made possible by a change of sign of the velocity. The part of the edge surface downstream of a line of parabolic edge points is thus mirrored with respect to the origin. It may be noted that as a consequence of the convention adopted for the sign, ϱ_1 changes sign when mirrored; thus elliptic edge points become hyperbolic edge points and vice versa. Along with the reversal of the streamline, the acceleration goes to infinity, as may be concluded from (117), and the radius of curvature of the spatial streamline goes to zero. It may be noted that on the edge surface the geodesic torsion of a curve tangent to the major principal direction is a property which has an equivalent significance as the direction of a curve at points on the hodograph surface for finite K_G. It is seen from equations (103) and (111) that only when $\varrho_1\to\infty$ are the geodesic torsions of the hodograph streamline and of the characteristic tangent to it equal to each other. This is equivalent to the tangency of the hodograph streamline and characteristic at an ordinary parabolic point. If $\tau \neq 0$, the line of parabolic edge points is seen to be the image of a conical limit line of the first type in a conical simple wave flow. Since the image of the line of parabolic edge points is tangent to a straight characteristic, as is the case for ordinary parabolic points, the following situations may prevail. In an expanding simple wave flow the conical limit line is inclined along the upstream straight characteristic direction on the concave side of the streamline or along the downstream straight characteristic direction on the convex side of the streamline. In a compressing simple wave flow the conical limit line is inclined along the downstream straight characteristic direction on the concave side of the streamline or along the upstream straight characteristic on the convex side of the streamline. From equation (67) it is seen that the same conclusions with regard to the variation of M_c along the streamline hold as for an ordinary conical limit line of the first type.

Singular points on a conical limit line in a conical simple wave flow arise at those points where τ becomes zero, and singularities similar to those for ordinary conical limit lines may be found.

Of special interest again is the situation where τ vanishes all along the space curve, which thus is a plane curve. The line of parabolic edge points then coincides with a streamline along which all normals to the edge surface fall in the direction of the binormal to the space curve. A point on the unit sphere is thus mapped onto a line on the edge surface. From equation (117) it follows that at this point the acceleration along the streamline becomes infinite. Also the acceleration normal to the streamline becomes infinite, and the radius of curvature of the physical streamline becomes zero. The physical streamline has a corner at the image point of the line of parabolic edge points, and the flow may be recognized to be a centered simple wave flow. The image point is the center of the straight characteristics. Such a singularity may be met, for example, in the flow around a supersonic leading edge of a flat delta wing at incidence in a homogeneous supersonic flow.

A conical simple wave flow may be bounded by an analytically different region along a characteristic, which, incidentally, may be a conical limit line of the second type.

Along a straight physical characteristic the simple wave flow may be bounded by a conical-supersonic parallel flow, since also in such a flow the characteristics are straight. The edge surface in the hodograph space then ends at a (conical) point of the hodograph surface. We discuss parallel flow in the next section.

If the conical simple wave flow is bounded by a curved characteristic, the edge surface is along a conical characteristic connected with a hodograph surface, which may have elliptic, parabolic or hyperbolic points along this line. Streamlines may enter or leave the edge surface from or to the hodograph surface, corresponding to flow into or out of a region of simple wave flow. They may be obtained from each other by flow reversal. Consider now a streamline at an elliptic point on the hodograph surface going onto an edge surface, and for example let the flow be as given in Fig. 6a. The streamline on the hodograph surface has a direction given by $\beta = 0$ and deflects to the characteristic angle arc tan $\pm\sqrt{M_c^2-1}$ when entering the edge surface. Since $g_s>0$, from (60) follows $\varrho_1>0$ and $\varrho_2>0$ for an elliptic point; thus $(\varkappa_n)_{\text{char.}}>0$, and at the point of the edge surface $\varrho_1>0$. The acceleration in the conical simple wave flow is thus positive, which is in accordance with the direction of the hodograph streamline when the edge surface coincides with a downstream hodograph characteristic. If the edge surface is taken along an upstream part of such a characteristic, the flow should decelerate; thus $g_s<0$, and $\varrho_1<0$. This conclusion may be obtained by mirroring the edge surface with respect to the origin. The edge surface point thus becomes a hyperbolic edge surface point, and a conical limit line of the second type occurs. By inspection of Figs. 5 and 6 and by similar arguments involving the signs of ϱ_1, ϱ_2 and g_s it may be shown more generally that the following rule holds.

If the streamline at an elliptic or hyperbolic point on the hodograph surface enters a region of conical simple wave flow, the edge surface of which coincides with a downstream hodograph characteristic, the transition from one type of flow to the other will be continuous, while if this surface coincides with an upstream characteristic, a conical limit line of the second type occurs. It may easily be verified that for elliptic points the interchange of downstream and upstream characteristics involves a change in the sign of the acceleration. Continuous transition then occurs if the simple wave flow and the neighboring flow are both expanding or compressing flows, while limit lines appear if one of the types of flow is expanding and the other compressing.

8. Regions of parallel flow in a conical flow field

Another singularity in the transformation occurs when the flow is parallel in a region of the conical flow field. Since the flow is conical, this region will be a cone, and the shape of this cone and the flow adjacent to it are of interest. If the parallel flow is conical-supersonic, it may be bounded by straight conical characteristics or the envelope of such conical characteristics, being a circular conical-sonic line. If the parallel flow is conical-subsonic, the boundary may be obtained by considering the hodograph transformation.

The region of parallel flow is mapped into the hodograph space at a point, and $\Delta\to\infty$. The hodograph surface, which is the representation of the adjacent flow field, exhibits a point where, depending on the way this point is approached along this surface, a different normal is found; this point is a conical point, and $K_G\to\infty$*. The cone of the normals at a conical point is congruent with and has the same position in space as the cone bounding the region of parallel flow. Now if the conical point is approached on the hodograph surface in a direction corresponding to the U direction of an arbitrary normal at this point, it is seen that R_V vanishes with respect to R_U, and it follows from the curvature relation, equation (36), that $M_c=1$. The tangent cone at the conical point thus

* An exception occurs if the parallel flow is entirely bounded by straight conical characteristics, in which case the normal at the point takes on different values because edge surfaces end at the point. The point is then not conical, and $M_c\neq 1$ in general. An example of such a situation is found in the interaction of conical simple waves, as studied by GIESE & COHN [*13*].

coincides with the characteristic cone of that point in the hodograph space, the axis of which is aligned along the velocity vector q and the semivertex angle of which is equal to arc tan $\sqrt{M^2-1}$. The normal cone is therefore a circular cone or a part of it, aligned along the velocity vector q and with a semi-vertex angle equal to $\mu = \text{arc tan}\,(M^2-1)^{-\frac{1}{2}}$. In the physical space the boundary is thus the upstream or downstream pointing Mach cone of the velocity in the parallel flow with apex at the center of the conical field, or a part of such a circular cone continued by a plane tangent to it along the generator where the two figures meet. Obviously, the planes corresponding to a figure composed of straight conical characteristics may also be a boundary of the parallel flow. The parallel flow may either be downstream or upstream of this boundary.

From EULER'S theorem (24) it follows that if the radius of curvature in any direction approaches zero, one of the principal radii of curvature must be zero; thus $\varrho_2 \to 0$, and DUPIN'S indicatrix degenerates to the point $\sqrt{|\varrho_1|}$ on the major principal axis and the point $\sqrt{|R|}=0$. The direction of the major principal axis is along the U axis, since $\varrho_2/\varrho_1 = 0$ and $M_c = 1$; thus $\alpha_1 = \beta = 0$. As for conical simple wave flows it may be shown by (108) and (111) that the conical streamlines map into each other. The same may be shown by equations (108) and (103) for the conical characteristics.

In order to investigate the properties of the flow adjacent to the parallel region, it will be assumed that the surface in the neighborhood of the conical point may be expressed by a series expansion, the first three terms of which can be written as

$$w = q + A(\Psi)\,p + B(\Psi)\,p^2. \tag{118}$$

A co-ordinate system is thus used which may be obtained by rotating the u, v and w axes until the w axis is along the velocity vector q in the parallel flow and u and v are replaced by $u = p\cos\Psi$ and $v = p\sin\Psi$. The velocity component normal to q is thus denoted by p. In these co-ordinates the differential equation (18) reads:

$$\begin{aligned} &w_{pp}\Big[1+\frac{1}{p^2}\,w_\Psi^2\Big(1-\frac{w^2}{a^2}\Big)\Big]+\frac{2}{p}\,w_{p\Psi}\Big[-\frac{1}{p}\,w_p\,w_\Psi\Big(1-\frac{w^2}{a^2}\Big)+\frac{p\,w}{a^2}\,\frac{1}{p}\,w_\Psi\Big]+\\ &+\frac{1}{p^2}\,w_{\Psi\Psi}\Big[1-\frac{p^2}{a^2}-2\,\frac{p\,w}{a^2}\,w_p+w_p^2\Big(1-\frac{w^2}{a^2}\Big)\Big]+\frac{1}{p}\,w_p\Big(1-\frac{p^2}{a^2}\Big)-2w_p^2\,\frac{w}{a^2}- \\ &-\frac{2}{p^2}\,w_\Psi^2\,\frac{w}{a^2}+\frac{1}{p}\,w_p^3\Big(1-\frac{w^2}{a^2}\Big)+\frac{2}{p^3}\,w_p\,w_\Psi^2\Big(1-\frac{w^2}{a^2}\Big)=0. \end{aligned} \tag{119}$$

Substituting equation (118) into (119) and collecting terms of the same order yields the following differential equations for the functions $A(\Psi)$ and $B(\Psi)$:

$$[A+A'']\,[1+A^2(1-M^2)]=0, \tag{120}$$

and

$$\begin{aligned} &[1+A^2(1-M^2)]\,B''-2A\,A'(1-M^2)\,B'+\\ &+2\,[2+\{3A^2+A'^2+2A\,A''\}\,(1-M^2)]\,B-\\ &-\frac{1}{q}\,M^2A(A+A'')\,[A^2\{2+(\gamma-1)\,M^2\}+2]=0, \end{aligned} \tag{121}$$

where M is the Mach number in the parallel flow, represented by the point $w=q$, $p=0$.

Solution of equation (120) yields two results, namely,

$$A(\Psi)=A\sin(\Psi-\Psi_0), \tag{122}$$

corresponding to a point on the hodograph surface which has a tangent plane, and

$$A(\Psi)=A=\pm\frac{1}{\sqrt{M^2-1}}, \tag{123}$$

which corresponds to a point on the hodograph surface with a tangent cone. As before, we again see that the tangent cone is a circular cone with semi-vertex angle arc tan $\sqrt{M^2-1}$ and with its axis along the velocity vector q of the parallel flow.

For a conical point equation (121) simplifies by use of (123) to

$$B(\Psi)=B=-\frac{\gamma+1}{2q}\,\frac{M^4}{(M^2-1)^2}. \tag{124}$$

Thus to a second approximation the hodograph surface is axially symmetric in the vicinity of the conical point. Correspondingly, the flow adjacent to the parallel flow is axi-symmetric in the immediate neighborhood of the Mach cone of the parallel flow. An analogous result was obtained by BULAKH [*18*], [*20*].

Furthermore, it is seen from (124) that a plane through q cuts the hodograph surface along a line of intersection which is concave towards the velocity vector q for $|w|<q$ and convex towards this axis of the tangent cone for $|w|>q$. From this fact the possible types of conical flow with a region of parallel flow may be obtained. They are sketched in Fig. 10. In this figure the possible meridian cuts of the hodograph surface are given. The corresponding physical flow patterns may be constructed by noting that the normal to the hodograph surface should be taken positive in the direction such that passing along the hodograph streamline and the corresponding physical streamline does not lead to contradictory results. It is seen that continuous transition from or into a parallel flow is possible across a downstream Mach cone if the adjacent flow is expanding (type I) and across an upstream Mach cone if the adjacent flow is compressing (type II). Transitions from or into a region of parallel flow across a downstream Mach cone if the adjacent flow is compressing (type III) and across an upstream Mach cone if the adjacent flow is expanding (type IV) are possible only if the hodograph surface is mirrored with respect to the origin. Thus in these cases conical limit lines of the second type occur. In Fig. 10 flows into a parallel flow region are denoted by *a* and flows out of such a region by *b*. Furthermore, it may be noticed that the types of flow IIb, IIa, IVb and IVa may be obtained from the types Ia, Ib, IIIa and IIIb, respectively, by flow reversal.

Further properties of the adjacent flow may be derived from the actual value of B, which yields for the major principal radius of curvature at a conical point the formula

$$\varrho_1 = \pm \frac{a}{\gamma+1} \sqrt{M^2 - 1}, \tag{125}$$

where the positive sign should be taken in expanding flow and the negative sign in compressing flow. From the approximate axial symmetry of the hodograph

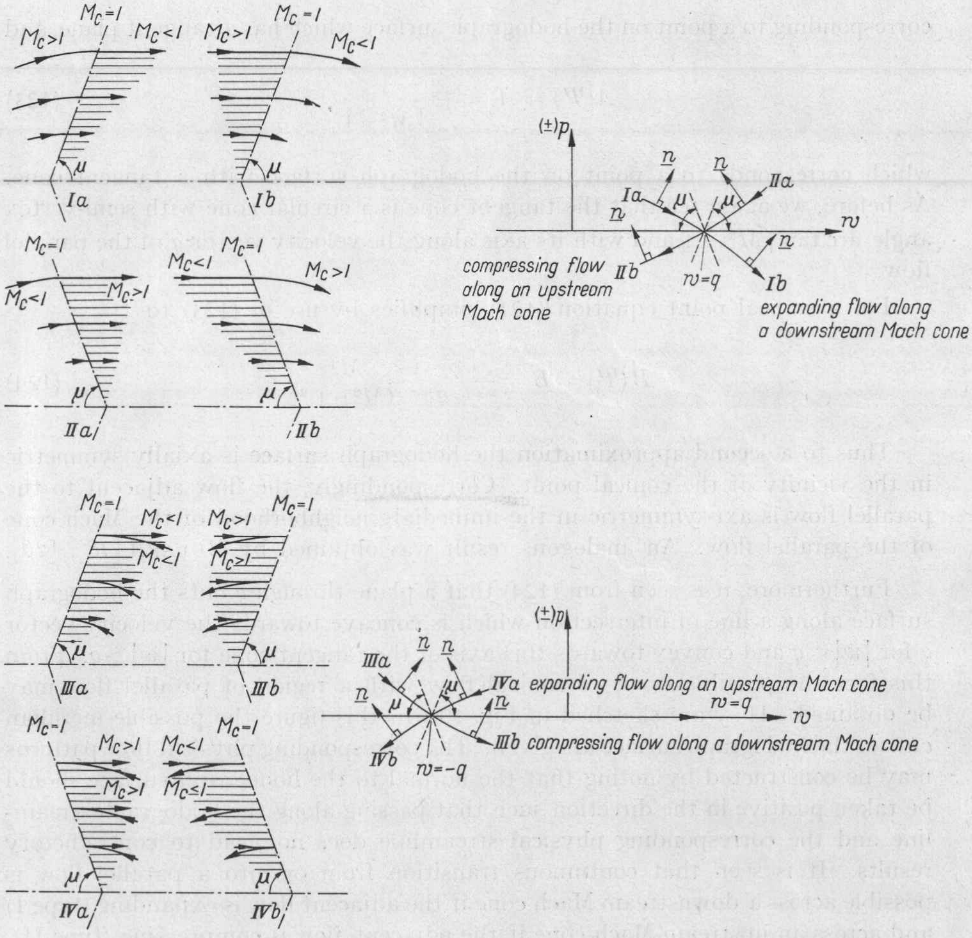

Fig. 10 a and b. Types of conical flow with a region of parallel flow. a) Continuous transition from or into a region of parallel flow, b) transition from or into a region of parallel flow across a limit cone.

surface in the neighborhood of the conical point the sign of ϱ_2 may be obtained, and so also the sign of the Gaussian curvature. Since $\beta = 0$ at the conical point, an elliptic point corresponds to conical-supersonic flow, and a hyperbolic point to conical-subsonic flow. Inspection of the meridian curves, given in Fig. 10, then shows that for a continuous transition the flow goes through $M_c = 1$, while across a limit cone the flow remains conical-subsonic or conical-supersonic.

This result may also be obtained by considering the variation of M_c along the streamline. In order to use equation (67) the acceleration along the streamline may be found from (60) and (125) to be

$$g_s = \pm \frac{a^2}{(\gamma+1)\,r} \frac{\sqrt{M^2-1}}{M}, \tag{126}$$

and, incidentally, the acceleration normal to the streamline may be obtained from equations (62) and (125):

$$g_n = \frac{a^2}{(\gamma+1)\,r} \frac{M^2-1}{M}, \tag{127}$$

while the radius of curvature of the physical streamline is equal to

$$R = (\gamma+1)\,r \frac{M^2}{M^2-1}. \tag{128}$$

The variation of M_c along the streamline is then equal to

$$\left(\frac{dM_c}{dU}\right)_s = -\frac{\gamma+1}{2a}, \tag{129}$$

which is exactly the negative of the value found at a parabolic point for $M_c = 1$, equation (91). Thus, in contrast to the case for parabolic points, where the local flatness of the hodograph surface leads to flow patterns with a close resemblance to two-dimensional plane flows, the infinite Gaussian curvature here leads to opposite tendencies. In fact, (129) shows that M_c decreases in an expanding flow and increases in a compressing flow*.

Since $M_c = 1$ at the Mach cone, the same conclusions as given above with regard to the change of M_c across this cone are then obtained.

The foregoing discussion permits some conclusions with regard to the existence of a second conical-sonic line, as discussed first by Ferri [17] and later by Bulakh [22].

In [17] the supersonic flow around a triangular conical wing with sharp supersonic leading edges and a flat outboard region was discussed. It was shown by means of a series expansion in the vicinity of the conical-sonic line and by numerical calculations that adjacent to the conical-supersonic parallel flow in the outboard region another conical-supersonic region existed, terminated by a second conical-sonic line. Since it may be expected that in this case the flow will be expanding behind the downstream Mach cone considered, type Ib of the flows just discussed will prevail, giving a conical-subsonic flow in the adjacent region. As was shown by Bulakh [22], the series expansion used in [17] was not valid in this case, so that conclusions can not be based on it. Also, Bulakh showed that in the rotational part of the flow field the conical streamlines are characteristics along which discontinuities in the derivatives of the velocity are possible. Such discontinuities actually occur along the conical streamline which

* At elliptic and hyperbolic points the Gaussian curvature is finite and different from zero, and both tendencies occur simultaneously, which is expressed by the fact that the sign of the variation of M_c is not determined by the sign of the acceleration alone.

separates the rotational from the irrotational flow, and along which the jump of vorticity, introduced by the discontinuity in the curvature of the shock wave, is carried downstream. Most likely these discontinuities were not accounted for in the numerical calculations. It may also be noticed that in several of the flow patterns given in [*17*] the conical-sonic lines on the convex body surfaces are inclined downstream instead of upstream as would follow from the previous discussion on conical-sonic lines.

If the transition from or into the parallel flow is continuous, the foregoing considerations, resulting in flows sketched in Fig. 10, show that a conical-supersonic flow adjacent to a parallel flow is possible in an expanding flow in front of a downstream Mach cone (type Ia) and in a compressing flow behind an upstream Mach cone (type IIb). Actually the latter type of flow may be found in the well known Busemann diffuser flow [*11*]. These flows will in general be bounded by another conical-sonic line.

If the transition occurs across a limit cone, Fig. 10 reveals that a conical-supersonic flow adjacent to a parallel flow occurs in compressing flow if the Mach (limit) cone is downstream with respect to the parallel flow (type IIIb) and in expanding flow if the Mach (limit) cone is upstream with respect to the parallel flow (type IVa).

The foregoing discussion does not pretend to give a complete analysis of the singularities in the transformation. For example, the properties of the transformation if $a \to 0$, both when $U \neq 0$ and when $U \to 0$, deserve further attention. Also, the existence of branch type singularities, where possibly the hodograph surface forms an edge line along which two sheets on the same side of this line meet, may be investigated.

It is hoped, however, that the consideration of the local properties of the hodograph transformation for irrotational conical flow from the point of view of differential geometry may have proved to give valuable information on the structure of conical flow. Nevertheless, the solution of a particular flow problem can be completed only by numerical calculation. Such a calculation may be performed either in the physical space, using a numerical method as described in the references cited above, or in the hodograph space. It would be useful to construct both the flow field and the hodograph surface while performing these calculations.

As an example of how the qualitative nature of the flow may be determined by means of the hodograph transformation, the flow around a flat delta wing with supersonic leading edges will now be discussed.

9. Supersonic flow around a flat delta wing with supersonic leading edges

An example of the flow around a delta wing with supersonic leading edges was first computed in the non-linear theory by Maslen [*14*] and since then has been given special attention by Fowell [*15*] and Bulakh [*21*]. Recently, Brook [*29*] also gave a discussion of the flow field. Consider a flat delta wing with semi-vertex angle δ, placed at an angle of attack α and zero yaw in a uniform supersonic stream with a Mach number M. The leading edges will be chosen to be supersonic; that is, $\delta > \arctan \sqrt{M^2-1}$ for α not too large. Take the origin of the right-handed co-ordinate system at the center of the conical flow, which is the apex of the wing, and the x and y axes in the plane of the wing, the x axis along the center line of the wing, positive in the downstream direction, and the y axis perpendicular to it, positive on the starboard side of the wing. The z axis is normal to the wing surface, and the angle of attack α is chosen positive if the positive z axis is on the upper side of the wing. A sketch of the flow field and the hodograph surface is given in Fig. 11. All curves and points on the unit sphere are projected centrally from the center of the conical flow onto a plane normal to the center line of the wing. The flow corresponds approximately to $\alpha=5°$, $\delta=45°$ and $M=3$.

Since the leading edges are supersonic, the flow on the upper and lower surface of the wing do not interfere and may thus be treated independently.

Consider first the upper side of the wing, where the flow is expanding around the leading edges. As sketched in Fig. 1 the conical characteristics are straight in the parallel flow. The region of flow influenced by the wing is bounded by the downstream part $B'C'$ of the conical characteristic through the point of intersection of the leading edge with the unit sphere and by the remaining part of the conical-sonic line, being the envelope of the straight conical characteristics in the parallel flow (which is not a characteristic curve as stated in [21]). The parallel flow is given on the hodograph surface by the point P_1 with the velocity vector $q=0.802$*, corresponding to $M=3$, pointing upwards at an angle of 5° with the u, v plane. The cone of the normals to the hodograph surface in P_1 is also sketched in Fig. 11. Adjacent to the straight characteristic $B'C'$ the flow will be a simple wave flow, and since at C' the conical physical streamline exhibits a corner, the flow is centered in C'. In order for the streamlines in the parallel flow to turn around the leading edge they should have their concave side towards the wing surface, so that the straight characteristics are inclined downstream on the convex side of the streamlines; the flow is thus expanding. The flow expands until the velocity vector is parallel to the wing surface and another region of parallel flow in between the last characteristic of the simple wave flow $C'F'$ and the wing surface occurs. This parallel flow region maps onto the point P_2 in the hodograph space. The conical simple wave flow is given in the hodograph space by an edge surface, lying in the plane through P_1 normal to the leading edge of the wing $O'C'$, and extends from P_1 to P_2. The curve coinciding with the edge surface is thus a plane curve, the binormal of which at every point is parallel to $O'C'$. The line of parabolic edge points corresponds to conditions in the center C' of the expansion waves, where, as was discussed before, the acceleration is infinite and the radius of curvature of the streamline is zero. Since the flow is expanding, the edge surface contains only elliptic edge points. The radius of curvature of P_1P_2 may be obtained from equation (115) when the velocity is resolved into its components along the tangent, normal and binormal of the space curve P_1P_2. Since P_1P_2 is a characteristic, the velocity component q_t along it is sonic. From (2) it follows, when $\gamma=1.4$, that

$$q_t^2=a^2=\frac{\gamma-1}{2}(1-q^2)=0.2-0.2q^2. \tag{130}$$

* Throughout this discussion the maximum speed will be taken as unity.

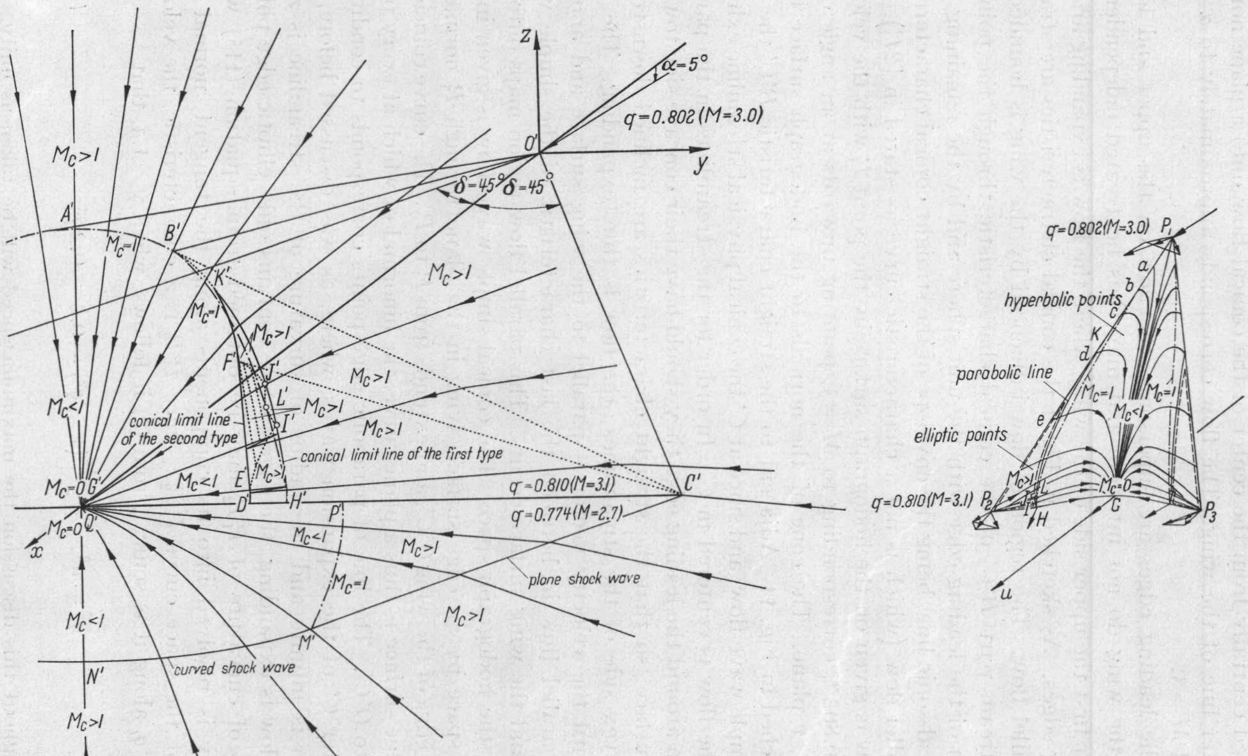

Fig. 11. Supersonic flow around a delta wing with supersonic leading edges

Furthermore, the velocity component along the binormal q_b may be found by projection of the velocity in P_1. Thus

$$q_b^2 = (0.802 \cdot \cos 5^\circ \cdot \cos 45^\circ)^2 = 0.3192. \tag{131}$$

For the velocity component along the principal normal q_n then follows

$$q_n = -\sqrt{q^2 - q_t^2 - q_b^2} = -\sqrt{1.2q^2 - 0.5192}, \tag{132}$$

and by (115) the radius of curvature of $P_1 P_2$ is given by

$$\varrho = 0.834\sqrt{1.2q^2 - 0.5192}. \tag{133}$$

Starting at P_1 in the direction normal to the plane $O'B'C'$, the curve $P_1 P_2$ may now be constructed*. The point P_2 then appears to have a velocity vector $q = 0.810$, corresponding to $M = 3{\cdot}10$ and deflected towards the center line of the wing through an angle of approximately 3°. From (117) it may be seen that along the first characteristic $B'C'$ the acceleration increases in the direction from B' to C' with the inverse of $\sin\vartheta$ to become infinite at C'. In B', $M_c = 1$; thus $U = a = q_t$, and $W = \sqrt{q^2 - U^2} = \sqrt{q_b^2 + q_n^2}$, from which it follows that $q_n (\sin\vartheta)^{-1} = W = a\sqrt{M^2 - 1}$. The acceleration along the streamline in B' then is shown from (117) to be equal to

$$g_s = \frac{2a^2}{(\gamma+1)\,r} \frac{\sqrt{M^2-1}}{M} = 0.0565\,\frac{1}{r}. \tag{134}$$

This is exactly twice the value of the acceleration in the flow adjacent to the conical-sonic line $A'B'$, which may be seen from (126) to be

$$g_s = \frac{a^2}{(\gamma+1)\,r} \frac{\sqrt{M^2-1}}{M} = 0.0283\,\frac{1}{r}. \tag{135}$$

The difference in nature of the simple wave flow, determined completely by the leading edge having a two-dimensional character, and the flow adjacent to the Mach cone of the undisturbed stream, influenced by the apex of the wing and having a three-dimensional character, is thus expressed by a jump in the acceleration in B'. It may be recalled that in the linear theory there is a discontinuity in the velocity across $B'C'$, while along $A'B'$ the velocity gradient in the bordering flow becomes infinite [*6*].

The influence of the apex of the wing, noticeable along $A'B'$, enters the simple wave flow at the point B' and carries downstream along the downstream conical characteristic $B'F'$. This boundary was also taken in the solution of MASLEN [*14*] and given special attention by BULAKH [*21*] when commenting on a paper by FOWELL [*15*]. It was pointed out by FOWELL [*15*] that it should

---

* It should be noted that $P_1 P_2$ is not the Prandtl-Meyer epicycloid shrunk by the factor $\sqrt{1 - q_b^2}$, as is stated in [*13*] in relation to centered simple wave flow around a swept-forward leading edge.

also be possible to construct the region of influence of the apex of the wing in the spatial flow field by considering the characteristic surface which emanates from the apex and intersects the unit sphere along a conical-sonic line. This line was then taken as boundary of the region of influence. As was noted in Section 2, however, disturbances originating at the apex of the wing admittedly travel initially along this characteristic surface but then continue along the characteristic surfaces from points on it. The envelope of these surfaces intersects the unit sphere along the above-mentioned conical characteristic $B'F'$*. In the hodograph space the shape of this characteristic is obtained from the known shape of P_1P_2 and the normal at P_1 corresponding to B' (direction $O'B'$). With the aid of (103) the normals to the edge surface along the image of characteristic $B'F'$ may then be determined, starting from the known values of M_c and $(\varkappa_n)_{\text{char.}}$ at P_1. The boundary between the parallel flow in the outboard region of the wing and the inboard region is the continuation of the characteristic $B'F'$ downstream along the straight characteristics $F'E'$. This boundary was also given by Maslen [*14*] and Bulakh [*21*]. It was pointed out by Bulakh [*21*] that in addition to this line the conical-sonic line $E'D'$ to which $F'E'$ is tangent concludes this boundary line, because when the angle of attack is decreased, the inboard region would otherwise fill the whole space influenced by the total wing. This argument, however, applies only to small angles of attack, for which a conical-sonic line $E'D'$ indeed may be expected, but the example given by Maslen and several numerical calculations presented by Brook [*29*] show that at higher angles of attack the straight characteristic continues up to the wing surface**.

It is natural to assume that the flow in the inboard region in the vincinity of the downstream Mach cone $A'B'$ is expanding, and the transition across the conical-sonic line will then be continuous since flow of the type Ib occurs. Thus, there is no ground to expect a shock wave to be formed near this line, as was done by Bulakh [*21*]. Along $A'B'$ the flow becomes conical-subsonic, and on the hodograph surface points close the conical point P_1 are hyperbolic. Because of the symmetry of the flow with respect to the line $A'G'$, the streamline $A'G'$ will not be curved out of the plane of symmetry; thus $\beta=\alpha_1=0$. On the image of the streamline $A'G'$ on the hodograph surface P_1G there will be hyperbolic points, where conditions as sketched in Fig. 3a prevail. The point G' is a conical stagnation point, where all the streamlines on the upper side of the wing come together, and it is mapped onto the orthogonal hyperbolic point G in the u, v plane. In the vincinity of the other downstream Mach cone $D'E'$ the flow may be assumed to be compressing. This may be justified by noting that in the parallel flow along the wing surface the streamlines are directed towards the center of the wing and have to be deflected to become parallel to it. Thus the streamlines must be curved with the concave side to the leading edge,

* Another conical flow solution where the region of influence of the origin has been incorrectly chosen was given in [*30*], where the supersonic flow near the junction of two wedges was studied.

** In the case that a conical-sonic line $D'E'$ appears, in [*29*] the characteristic tangent to $D'E'$ in D' is incorrectly taken as the boundary between the regions determined by the leading edge and the wing apex.

and the pressure gradient is therefore opposite to the direction of flow (and lying in the x, y plane, normal to the radius). Stated more freely, the two-dimensional expansion around the leading edge would be too severe for a three-dimensional flow, and as soon as the influence zone of the apex is reached, it appears that an overexpansion has taken place which has to be neutralized by a compression. From the considerations given in the section on parallel flow it follows, however, that the transition to compressing flow along a downstream Mach sone leads to flow type IIIb, such that the Mach cone is a limit cone. The curve $D'E'$ is therefore, for all angles of attack, a conical limit line. The flow near $D'E'$ in the inboard region is conical-supersonic. Since the streamline $D'G'$ along the wing surface is not curved out of the x, y plane, it follows that $\beta=0$, and on the hodograph surface $D'H'$ is mapped onto a curve of elliptic points P_2H lying in the u, v plane where conditions as sketched in Fig. 6d prevail. In order for the streamline to arrive at G' it should return once more, while since $M_c=0$ in G', the flow should change from conical-supersonic to conical subsonic. Since $\beta=0$ all along the streamline on the wing surface, the latter means also that on the hodograph surface at the same point the points along the hodograph streamline change from elliptic to hyperbolic. This transition occurs at the parabolic point H, where since $\beta=0$, $M_c=1$ (Fig. 7d), while the image point H' is a point of a conical limit line of the first type. The streamline $H'G'$ is mapped onto the line of hyperbolic points HG in the u, v plane, where conditions exist as given in Fig. 3e. Along P_2GP_3 the hodograph surface is normal to the u, v plane. At H the parabolic line is normal to the u, v plane, while at H' the conical limit line is normal to the x, y plane. On the hodograph surface the parabolic line runs to some point K, and the whole of this surface containing elliptic points (excluding the elliptic edge points on P_1P_2) is mirrored with respect to the origin. In Fig. 11 the area to be reflected is enclosed by a dotted line. Evidently, the disturbance introduced at B' propagates along the downstream characteristic $B'E'$ and the conical sonic line $E'D'$ in such a way that downstream of some point K' a conical limit line of the second type is formed. The exact location of K' can be found only by a numerical calculation of the whole flow field. In fact, the hodograph surface, excluding the edge surfaces P_1P_2 and P_1P_3 only, contains regions where the differential equation is either elliptic, parabolic or hyperbolic, depending on an elliptic region. For reasons which will become apparent later, it will be assumed that K' lies on $B'F'$ somewhere in between B' and F'. The straight characteristic $F'E'$ is then a limit line. The flow adjacent to it must have straight characteristics and thus will be a conical simple wave flow. Furthermore, the waves will not be centered, because otherwise the flow would be completely determined by the outboard region. In the hodograph space this conical simple wave flow is mapped onto an edge surface P_2L, which coincides with a space curve, since its torsion is different from zero. In P_2 the tangent to P_2L is normal to the plane $O'E'F'$, and since the flow is decelerating, the edge surface consists of hyperbolic edge points, which are obtained by mirroring the edge surface containing elliptic edge points. The region of conical simple wave flow will be bounded by the curved downstream characteristics from E' and F', which arrive at their point of intersection L' as upstream characteristics. Since both characteristics are curved and only two characteristic directions are possible, the direction of the straight characteristic must coincide with at least one of them at L'; thus $M_c = 1$, and both curved characteristics are tangent to the straight characteristic. The edge surface P_2L therefore ends on the conical-sonic line which runs from H to the conical point P_1. Along $F'L'$ and $E'L'$ propagates a discontinuity in the acceleration, caused by the junction of a conical simple wave flow and an analytically different region. It will be assumed that along the limit line $H'K'$, H' is the only conical-sonic point. The point L' then lies downstream of $H'K'$, and the characteristic $F'L'$ and $E'L'$ intersect the limit line in J' and I', respectively. Since the transition across $F'J'$ occurs continuously, the image of the region $F'J'K'$ on the hodograph surface P_2JK consists of elliptic points, as do the edge surface in the region P_2IJ and the hodograph surface in the region P_2IH, which is the image of region $D'E'I'H'$ on the unit sphere. The parabolic line HK enters the edge surface at I and continues as a line of parabolic edge points IJ, leaving this surface at J to become a parabolic line JK again. The image of IJ on the unit sphere $I'J'$ is the envelope of straight characteristics.

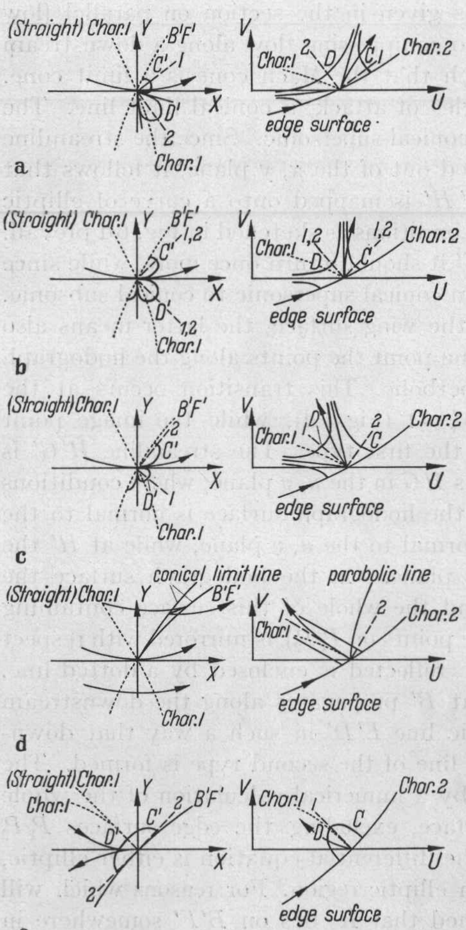

Fig. 12 a—e. Typical conditions on the characteristic $B'F'$

Conditions in the inboard region along $B'F'$ may be deduced from the hodograph surface by assuming that β varies continuously along the characteristic separating the edge surface P_1P_2 from the hodograph surface. Typical points along this curve are chosen in Fig. 12 to show the different situations which prevail. The image of the streamline through B' on the side of F' leaves the edge surface P_1P_2 in P_1 along the U axis, which is also the direction of P_1P_2 at this point, and $\beta = \alpha_1 = 0$, where $M_c = 1$. From B' to F' along $B'F'$, M_c increases; thus on the edge surface $|\beta|$ increases when going from P_1 to P_2. On the hodograph surface $|\beta|$ increases more rapidly, in accordance with the fact that at hyperbolic points the hodograph streamline should lie in the region which the hodograph characteristics enclose around a direction normal to the U axis. It follows then that at these points the flow is still expanding if $|\beta| < \frac{1}{2}\pi$, as sketched in Fig. 12a, and when $|\beta|$ is increased more, the acceleration along the streamline becomes zero for $|\beta| = \frac{1}{2}\pi$ (Fig. 12b), while the flow is compressing if $|\beta|$ exceeds this value (Fig. 12c). In all these cases the transition across $B'F'$ is continuous, since if the flow is reversed, the streamline on the edge surface is seen to be directed along the downstream characteristic*. Thus in the neighborhood of B' in addition to the small two-dimensional expansion a spatial expansion occurs, and further downstream along $B'F'$, a continuous compression. If $B'F'$ is followed further downstream, $|\beta|$ changes enough to bring the streamline into the other characteristic direction when the parabolic point K is reached. The deceleration has then become infinite, and the situation is sketched in Fig. 12d. It may easily be shown, from the transformation, that the conical limit line of the first type in K' touches the characteristic $B'F'$, which from this point on becomes a conical limit line of the second type. Still further downstream the hodograph streamline enters the region which the characteristics enclose around the U axis, and the point is thus elliptic, which also may be deduced from the fact that the parabolic line is crossed. The transition is now across a limit line, since if the flow is reversed, the streamline on the edge surface is directed along the upstream characteristic, while the flow changes from expanding to compressing. This situation is sketched in Fig. 12e. The course of the physical conical streamlines and the hodograph streamlines on the expansion side of the wing may now easily be understood from the considerations given above.

Because of the appearance of limit cones at all angles of attack it may be concluded that no continuous solution for the flow on the expansion side exists**. In order that a physically possible flow pattern can occur, in the region of the limit cones a shock wave must be formed. The formation of this inboard shock may be expected to start with zero strength at the point K' tangent to the two limit cones and to continue until it hits the wing surface normally***.

Indeed, as was shown by Fowell [*15*] in experiments, an inboard shock wave was found. The flow downstream of this shock wave does not necessarily have to be conical-subsonic, and it will be rotational if the shock is curved. In G' a Ferri singularity in the entropy distribution will then occur.

On the lower side of the wing a compression takes place, and an isentropic solution involving limit cones may also be constructed. Yet, obviously, unless detachment occurs, a plane shock wave $C'M'$ may be seen to be attached to the leading edge, downstream of which a region of flow parallel to the wing surface exists. This region of parallel flow is bounded downstream by a Mach cone, showing up as a circular conical-sonic line $M'P'$ on the unit sphere. Since

---

* This continuous transition may be shown not to be in contradiction with the fact that the characteristic separates regions of elliptic edge points and hyperbolic points, because the edge surface lies on the same side of this separation curve as the hodograph surface.

** This conclusion was also reached in [*15*] and [*29*], where it was remarked that the simple wave regions from the leading edges at some angle of attack overlap, thus making a continuous solution impossible. As was pointed out before, however, this picture of the flow is based on an incorrect presentation of the spatial influence of the apex of the wing and does not justify conclusions with regard to the possibility of a continuous solution.

*** In [*21*] and [*29*] it was assumed that the shock wave begins at D'. There is no reason, however, to expect that the shock will extend beyond K' in the region where a continuous transition across $B'F'$ was found.

in the parallel flow the streamlines are directed away from the wing center line, an expansion occurs along $O'P'$ in order to turn the streamlines towards the direction of the center line. The type of flow Ib therefore prevails, giving a continuous transition across $C'M'$ into a conical-subsonic flow. Thus, there is no reason to expect a shock wave to be formed in the neighborhood of $C'M'$ as was done by Bulakh [*21*]. In the example given by Maslen [*14*], along $C'M'$ the flow was found to be conical-supersonic. As was pointed out by Bulakh [*22*], however, the jump in curvature of the shock wave at the junction of the plane shock $C'M'$ and the curved shock $M'N'$ introduces a jump in vorticity, propagating downstream along the streamline $M'Q'$, which is most likely not accounted for in the numerical calculations in [*14*]. Since downstream of the curved shock the flow is rotational, a velocity potential cannot be defined, and the hodograph transformation breaks down. Also for this reason, the hodograph surface for the compression side of the wing is not given in Fig. 11. Again a Ferri singularity in the entropy distribution occurs at Q'.

This completes the present description of the supersonic flow around the delta wing with supersonic leading edges.

A note may be added concerning the supersonic flow around the tip of a flat rectangular wing at incidence, which was discussed in connection with the delta wing by Bulakh [*21*]. Since this flow pattern essentially may be obtained by turning one of the leading edges of a delta wing with 90° apex angle perpendicular to the undisturbed flow while the other then becomes a subsonic edge, the flow on the side of the leading edge may be expected to be similar to that for the delta wing as discussed before. In fact, it may be shown that on the expansion side two limit lines again appear, which are tangent at their point of contact on the characteristic terminating the Prandtl-Meyer expansion, and thus a continuous solution is not possible. Again an inboard shock will be formed, starting with zero strength at the point of tangency of the limit lines. On the compression side of the wing the parallel flow is again bounded by a downstream Mach cone along which a continuous transition into expanding flow takes place and no shock occurs. The hodograph surface for this flow pattern as given by Busemann [*23*] may be modified, according to the results found for the delta wing, to include regions of elliptic points, in which an edge surface is imbedded, and separated from the region of hyperbolic points by a parabolic line. The conditions on the subsonic edge are given by a parabolic line, coinciding with a characteristic, which also is a streamline.

Acknowledgement. The investigation presented above was carried out while the author was working at the Institute of Applied Mathematics. He is greately indebted to Prof. dr. R. Timman for his stimulating encouragement during the course of it and for reading the manuscript. The initial approach to the subject was made while the author was working with the Aeronautical Engineering Department, under the direction of Prof. dr. ir. H. J. v. d. Maas. He would also like to thank Dr. I. W. van Spiegel for interesting discussions.

References

[1] Busemann, A.: Drücke auf kegelförmige Spitzen bei Bewegung mit Überschallgeschwindigkeit. Z. angew. Math. Mech. **9**, 496—498 (1929).

[2] Heaslet, M., & H. Lomax: Generalized conical flow fields in supersonic wing theory. NACATN 2497, September (1951).

[3] Stewart, H. J., & A. J. Ormsbee: Conical techniques for incompressible nonviscous flow. J. Aeron. Sci. **23**, 1029—1036 (1956).

[4] Busemann, A.: Infinitesimale kegelige Überschallströmung. Schriften der Deutschen Akademie der Luftfahrtforschung 7B, H. 3, 105—122 (1943). Translated as NACATM 1100.

[5] Germain, P.: La théorie générale des mouvements coniques et ses applications à l'aérodynamique supersonique. ONERA, Publ. no. 34 (1949).

[6] Goldstein, S., & G. N. Ward: The linearized theory of conical fields in supersonic flow with application to plane airfoils. Aeron. Quart. II, 39—84, May (1950).

[7] Moore, F. K.: Second approximation to conical flows. J. Aeron. Sci. **17**, 328—334 (1950).

[8] Van Dyke, M. D.: First and second order theory of supersonic flow past bodies of revolution. J. Aeron. Sci. **18**, 161—178 (1951).

[9] Stone, A. H.: On supersonic flow past a slightly yawing cone. J. Math. and Phys. **27**, 67—81 (1948).

[10] Ferri, A., N. Ness & T. Kaplita: Supersonic flow over conical bodies without axial symmetry. J. Aeron. Sci. **20**, 563—571 (1953).

[11] Busemann, A.: Die achsensymmetrische kegelige Überschallströmung. Luftfahrtforschung **19**, No. 4, 137—145 (1942).

[12] Taylor, G. I., & J. W. Maccoll: The air pressure on a cone moving at high speeds. Proc. Roy. Soc., Ser. A **139**, 278—311 (1933).

[13] Giese, J. H., & H. Cohn: Two new non-linearized conical flows. Quart. of Appl. Math. **11**, 101—108 (1953).

[14] Maslen, St.: Supersonic conical flow. NACATN 2651, March (1952).

[15] Fowell, L. R.: Exact and approximate solutions for the supersonic delta wing. J. Aeron. Sci. **23**, 709—720, August (1956).

[16] Ferri, A., R. Vaglio-Laurin & N. Ness: Mixed-type conical flow without axial symmetry, Polytechnic Institute of Brooklyn, PIBAL Report 264, December (1954).

[17] Ferri, A.: Recent theoretical work in supersonic aerodynamics at the Polytechnic Institute of Brooklyn. Proc. of the Conf. on High-Speed Aeronautics, Pol. Inst. of Brookl., 20 January (1955).

[18] Bulakh, B. M.: On the theory of conical flows. Prikl. Mat. i. Mech. **18**, No. 4, 451—452 (1954). [In Russian.]

[19] Bulakh, B. M.: On the theory of non-linear conical flows. Prikl. Mat. i. Mech. **19**, No. 4, 393—409 (1955). [In Russian.]

[20] Bulakh, B. M.: On the theory of conical flows. Prikl. Mat. i. Mech. **21**, No. 1, 143—144 (1957). [In Russian.]

[21] Bulakh, B. M.: Remarks on Fowell's paper: Exact and approximate solutions for the supersonic delta wing. Prikl. Mat. i. Mech. **22**, No. 4, 404—407 (1958). [In Russian.]

[22] Bulakh, B. M.: Remarks on Ferri's article: Recent theoretical work in supersonic aerodynamics at the Polytechnic Institute of Brooklyn. Prikl. Mat. i. Mech. **23**, No. 3, 576—580 (1959). [In Russian.]

[23] Busemann, A.: Aerodynamischer Auftrieb bei Überschallgeschwindigkeit. Luftfahrtforschung **12**, 210—220 (1935).

[24] Giese, J.: Compressible flows with degenerate hodographs. Quart. Appl. Math. **9**, 237—246 (1951).

[25] Nikol'skii, A. A.: On a class of adiabatic gas flows which map on a surface in the hodograph space. CAHI, Moscow (1949). [In Russian.]

[26] Ryzhov, O. S.: On flows with a degenerate hodograph. Prikl. Mat. i. Mech. **21**, 564—568 (1957). [In Russian.]

[27] Strubecker, K.: Differentialgeometrie. Sammlung Göschen, Berlin 1959.

[28] v. Mises, R.: Mathematical Theory of Compressible Fluid Flow. New York: Academic Press Inc. Publishers 1958.

[29] Brook, J. W.: Non-linear supersonic conical flow over flat plate delta wings. Report RE-117, Grumman Engineering Corporation Research Department, May (1959).

[30] Hains, F. D.: Supersonic flow near the junction of two wedges. J. Aero./Space Sci. **25**, 530—531 (1958).

Druck der Universitätsdruckerei H. Stürtz AG., Würzburg

Overzicht

In dit proefschrift worden supersone wervelvrije kegelstromingen beschouwd. Dit zijn stromingen van een samendrukbaar medium (gas), waarvoor in ieder punt van de (driedimensionale) ruimte, de snelheid groter is dan de locale geluidssnelheid, geen wervels optreden en de toestandsgrootheden van het gas (bijv. de druk en de temperatuur) en snelheid constant zijn op stralen door het centrum van het kegelvormige veld. Het veld kan daarom worden beschreven op de eenheidsbol met het centrum als middelpunt. Door het ontbreken van wervels in de stroming kan een snelheidspotentiaal worden gedefinieerd, welke door toepassing van de wetten van de mechanica en thermodynamica blijkt te voldoen aan een partiële differentiaalvergelijking van de tweede orde met als onafhankelijk veranderlijken twee plaatscoördinaten, welke worden gebruikt om op de eenheidsbol te meten. Deze differentiaalvergelijking heeft een quasi-lineair karakter, d.w.z. de termen van de tweede orde komen voor in een lineaire combinatie, terwijl hun coëfficiënten echter afhangen van de onafhankelijk veranderlijken, eerste afgeleiden van de potentiaal en de potentiaal zelf. Het type van deze vergelijking in een bepaald punt op de eenheidsbol wordt bepaald door de waarde van het conische getal van Mach M_c, gedefinieerd als de verhouding van de snelheidscomponent loodrecht op de straal (dus voor een punt op de eenheidsbol, rakend aan de eenheidsbol) en de locale geluidssnelheid. Voor een conisch-subsone stroming ($M_c < 1$) is de vergelijking elliptisch, voor een conische-sonische stroming ($M_c = 1$) parabolisch en voor een conisch-supersone stroming ($M_c > 1$) hyperbolisch. De twee families karakteristieken van de vergelijking worden conische karakteristieken genoemd en liggen op het boloppervlak. Zij bepalen de twee karakteristieke richtingen in een punt van de bol, welke verschillend en imaginair zijn voor $M_c < 1$, samenvallend en reël voor $M_c = 1$ en verschillend en reël voor $M_c > 1$. De doorsnijding met de eenheidsbol van een kegel met het centrum als top en een (ruimtelijke) stroomlijn als richtkromme wordt conische stroomlijn genoemd. De samenhang van deze beschrijving van de stroming op de eenheidsbol en die in de ruimte, zowel als de overeenkomsten en de verschillen met de tweedimensionale vlakke stroming van een samendrukbaar medium worden besproken en toegelicht aan het voorbeeld van de homogene evenwijdige stroming.

Teneinde de structuur van kegelvormige velden nader te leren kennen worden vanuit één punt de snelheidsvectoren van een dergelijk veld uitgezet, zodat de eindpunten aldus een oppervlak opspannen in de hodograafruimte. De transformatie van de physische ruimte naar de hodograafruimte staat bekend als de, ook voor vlakke samendrukbare stromingen toegepaste hodograaf-of Legendretransformatie. Het blijkt nu, dat voor kegelstromingen de afbeelding van het hodograafoppervlak op de eenheidsbol in de physische ruimte de, uit de differentiaalmeetkunde bekende Gausse of spherische afbeelding van een oppervlak is. Dit wil zeggen, dat wanneer de eenheidsnormaalvectoren van het hodograafoppervlak worden uitgezet vanuit één punt, juist de voor de beschrijving van kegelstromingen gebruikte eenheidsbol in de physische ruimte wordt verkregen.

Er volgt nu een differentiaalmeetkundige beschrijving van het hodograafoppervlak en van de locale eigenschappen van de transformatie met behulp van een, uit de differentiaalvergelijking af te leiden relatie voor de kromstralen in een punt van het hodograafoppervlak. De afbeeldingsdeterminant van Jacobi voor de afbeelding van de bol op het hodograafoppervlak blijkt bijvoorbeeld gelijk te zijn aan de Gausse kromming van laatstgenoemde oppervlak (zo ook aan de verhouding van de oppervlakte van een oppervlakteelement op de bol tot dat van het corresponderende oppervlakteelement op het hodograafoppervlak). Voorts wordt aangetoond, dat de conische karakteristieken op het hodograafoppervlak een geconjugeerd net vormen, welke zich afbeeldt op het net van de conische karakteristieken op de eenheidsbol. Hieruit en uit de transformatie volgt dan, dat de conische karakteristieken op het hodograafoppervlak van één familie en de conische karakteristieken op de eenheidsbol van de andere familie een stelsel vormen, dat in de corresponderende punten orthogonaal is. Een ander geconjugeerd net op het hodograafoppervlak vormen de lijnen van constante grootte van de snelheid en de stroomlijnen. Een geconjugeerd net van krommen van belang als referentiesystem is het (orthogonale) net der krommingslijnen, welke zich op de bol afbeeldt, zodanig, dat in de corresponderende punten een kromingslijn evenwijdig is aan zijn afbeelding op de bol. Nadat, de physich van belang zijnde grootheden zijn uitgedrukt in meetkundige grootheden van het hodograafoppervlak, — zo kan bijvoorbeeld ook de versnelling van een gasdeeltje op eenvoudige wijze worden geschreven als de som van de hoofkromtestralen van het hodograafoppervlak in het corresponderende punt —, volgt een nader onderzoek van het gedrag van de hodograafstroomlijnen en karakteristieken t.o.v. de kromtelijnen, wanneer het conische getal van Mach M_c en de Gausse kroming (juister gezegd de verhouding van de hoofdkromtestralen en de som der hoofdkromtestralen) worden gevarieerd. Voor een reguliere afbeelding, dus wanneer de afbeeldingsdeterminant (of Gausse kromming) eindig en van nul verschillend is, en dientengevolge de punten op het hodograafoppervlak elliptisch of hyperbolisch zijn, wordt dit gedrag in detail besproken voor conisch-subsone, conisch-sonische en conisch-supersone stromingen en toegelicht aan een aantal figuren (figuur 3 *t/m* 6).

Singulariteiten in de afbeelding treden op wanneer de Gausse kromming naar nul of oneindig gaat, terwijl dan de hodograafstroomlijn en één van de conische karakteristieken beiden raken aan de kromtelijn, waarvoor de absolute waarde van de hoofdkromtestraal het grootst is. Zij treden dus op voor $M_c \geqq 1$.

Er wordt aangetoond, dat een lijn van parabolische punten de afbeelding is van een conische grenslijn (van de eerste soort) d.i. de doorsnijding van een kegelvormige grensoppervlak met de eenheidsbol. De mogelijkheid van het optreden van discontinuïteiten in tweede en hogere afgeleiden van de potentiaal langs de karakteristieken leidt tot het mogelijke bestaan van conische grenslijnen (van de tweede soort), welke worden afgebeeld op conische hodograafkarakteristieken, waarvoor de afbeeldingsdeterminant (Gausse kromming) door nul springt.

Een parabolische lijn, welke geheel samenvalt met een hodograafstroomlijn en hodograafkarakteristiek is de afbeelding van de stroming in het randpunt van de stroming om een scherpe rand, zoals bijvoorbeeld in de omstroming van een subsone vleugelvoorrand van een deltavleugel voorkomt.

Als voorbeeld van stromingen, waarvoor de afbeeldingsdeterminant naar oneindig gaat worden de stromingen besproken, waarvoor langs slechts één der families conische karakteristieken zich verstoringen voortplanten (simple wave flow). Deze stromingen worden afgebeeld in de hodograafruimte op een randoppervlak, d.i. een oppervlak, dat samenvalt met een ruimtekromme, terwijl in elk punt van de ruimtekromme verschillende punten van het randoppervlak, onderscheiden door hun normaal, samenvallen met dit punt van de ruimtekromme. Met behulp van de transformatie worden nu elliptische, parabolische en hyperbolische randpunten gedefinieerd en de eigenschappen van de transformatie verder onderzocht in analogie met het geval voor een eindige Gausse kromming. Een lijn van parabolische randpunten blijkt de afbeelding te zijn van een conische grenslijn (van de eerste soort) in een „simple wave" stroming. Een lijn van parabolische randpunten, welke geheel samenvalt met een hodograafstroomlijn en hodograafkarakteristiek is de afbeelding van het snijpunt met de eenheidsbol van de centreerlijn van een gecentreerde „simple wave" stroming om een scherpe rand, zoals bijvoorbeeld in de omstroming van een supersone vleugelvoorrand van een deltavleugel voorkomt.

De overgang van een „simple wave" stroming naar een stroming, waarin langs beide families karakteristieken verstoringen lopen wordt onderzocht, waarbij speciaal wordt gelet op het optreden van conische grenslijnen.

Een ander voorbeeld van het geval, waarvoor de afbeeldingsdeterminant naar oneindig gaat is dat van de homogene evenwijdige stroming, welke wordt afgebeeld op een punt in de hodograafruimte. De mogelijke begrenzingen van dit soort stromingen en de wijze van overgang naar aangrenzende kegelstromingen wordt onderzocht, waarbij weer in sommige gevallen grenslijnen worden gevonden.

Tot slot wordt als toepassing van bovenstaande beschouwingen aangegeven hoe door gelijktijdige constructie van het hodograafoppervlak en het veld op de eenheidsbol in de physische ruimte een kwalitatief beeld kan worden verkregen van de supersone stroming om een deltavleugel met supersone vleugelvoorranden, onder een invalshoek geplaatst in een homogene evenwijdige stroming. Dit beeld wordt vergeleken met uit de literatuur bekende numeriek berekende resultaten.

STELLINGEN

I

De door Lighthill gegeven schokgolfpatronen in de supersone stroming om een deltavleugel met subsone vleugelvoorranden en de supersone stroming om een tip van een rechthoeksvleugel kunnen met behulp van de, in dit proefschrift besproken mogelijke overgangen van en naar een gebied van evenwijdige stroming opnieuw worden geïnterpreteerd en aangevuld.

The shock strength in supersonic "conical fields",
M. J. Lighthill, The Philosophical Magazine, 1949, 1202-1223.

II

Voor de, door Bulakh beschouwde supersone stroming om een vleugel met voorwaartse pijlvorm is door hem het randwaardeprobleem voor de expanziezijde incorrect geformuleerd, waardoor het schokgolfpatroon ten dele onjuist is. Door constructie van het hodograafoppervlak met behulp van differentiaalmeetkundige beschouwingen van de hodograaftransformatie is een juist beeld van de samenhang van deze stroming te verkrijgen.

On the theory of non-linear conical flows,
B. M. Bulakh, Prikl. Mat. i. Mech. 19, No. 4, 393-409 (1955).

III

De bewering van Birkhoff en Walsh, dat de axiaalsymmetrische kegelstroming om een stroomafwaarts gepunte cirkelkegel (the jetless axially symmetric collapse) mathematisch niet mogelijk is, is onjuist.

Conical, axially symmetric flows, G. Birkhoff en J. M. Walsh,
Mémoires sur la Méchanique des Fluids, Paris, 1953.

IV

De wrijvingsloze, samendrukbare, axiaalsymmetrische stroming om een van achteren, met een van nul verschillende hoek, toegespitst omwentelingslichaam bezit in het achterste punt van het lichaam een stuwpunt.

Compressible inviscid flow near the end of pointed afterbodies,
J. W. Reyn, Journal of the Aero/Space Sci., Vol. 25, No. 12, 787, 1958.

V

Met enkele eenvoudige veranderingen zijn de, in dit proefschrift gegeven differentiaalmeetkundige beschouwingen, behalve voor gebieden met evenwijdige stroming, ook van toepassing op de hodograaftransformatie voor vlakke, samendrukbare, wervelvrije stromingen.

VI

Tegen de, door Tsien voorgestelde physische definitie van een grenslijn (-oppervlak) als de omhullende van de karakteristieken (karakteristieke oppervlakken) van één familie zijn bezwaren in te brengen. Het is beter deze te definiëren als een lijn (oppervlak), waarover de stroming niet kan worden voortgezet.

The "limiting line" in mixed subsonic and supersonic flow of compressible fluids, H. S. Tsien, NACA TN 961, 1944.

VII

In stationaire en instationaire compressibele stromingen in één, twee of drie dimensies kunnen, behalve de gewoonlijk in de literatuur besproken grenslijnen (oppervlakken), welke als omhullende van de ene familie karakteristieken (karakteristieke oppervlakken) en meetkundige plaats van de snavelpunten (keerranden) van de andere familie karakteristieken (karakteristieke oppervlakken) verschijnen, en waarvoor de afbeeldingsdeterminant voor de transformatie van de physische of plaatstijd ruimte naar de hodograaf- of karakteristieken ruimte nul wordt, grenslijnen (oppervlakken) worden gevonden als die delen van de karakteristieken (oppervlakken), waarover de afbeeldingsdeterminant discontinu door nul gaat, zonder dat de afbeelding van deze lijnen keerranden zijn.

VIII

Met behulp van de, in de vorige stelling genoemde grenslijnen is het mogelijk een goede beschrijving te geven van bijvoorbeeld de vlakke supersone stroming zonder schokgolven langs een concave wand, welke onder anderen in onderstaande boeken over gasdynamica onjuist wordt behandeld.

Supersonic flow and shock waves, R. Courant and K. O. Friedrichs, Interscience Publishers, Inc., New York, 1948, blz. 295.

General theory of high speed aerodynamics, Editor: W.Sears, Princeton University Press, Princeton, 1954, blz. 380.

Theorie schallnaher Strömungen, K. G. Guderley, Springer Verlag, Berlin/Göttingen/Heidelberg, 1957, blz. 93.

Mathematical theory of compressible fluid flow, R. von Mises, Academic Press, Inc., Publishers, New York, 1958, blz. 306.

IX

In de afleiding, welke door Courant en Hilbert wordt gegeven voor de differentiaalvergelijking, welke de voortplanting beschrijft van discontinuïteiten in de tweede afgeleiden u_{xx}, u_{xy} en u_{yy} van een functie $u = u(x, y)$, welke voldoet aan de quasi-lineaire differentiaalvergelijking
$a(x, y, u, u_x, u_y)u_{xx} + b(x, y, u, u_x, u_y)u_{xy} + c(x, y, u, u_x, u_y)u_{yy} + d(x, y, u, u_x, u_y) = 0$
is geen rekening gehouden met het feit, dat a, b, c en d, hoewel continu differentiëerbare functies van x, y, u, u_x en u_y niet differentiëerbaar zijn over de karakteristiek, zodat de vergelijking niet lineair is, zoals door hen wordt beweerd.

Methoden der Mathematischen Physik II, R. Courant und D. Hilbert, Verlag von Julius Springer in Berlin, 1937, 291-299.

X

Voor de, door Pivko beschouwde stroming met hoge snelheid om een slippende vleugel-romp combinatie met verticaal staartvlak is door hem het randwaarde probleem niet juist gesteld. Hierdoor bezit de gegeven oplossing niet de nauwkeurigheid van de theorie voor naaldvormige lichamen (Slender body theory) en is zijn waarde twijfelachtig.

Sur l'influence du fuselage sur l'aile et l'empennage vertical aux grandes vitesses, S. Pivko, Technique et Science Aéronautiques, 1955, 387-394.

XI

De groeiende betekenis van de wetenschappelijke en technische ontwikkeling in de Sowjet-Unie maakt het noodzakelijk, dat het Westen beschikt over wetenschapsmensen en technici, die de Russische literatuur kunnen volgen. Nederland kan hiertoe bijdragen door het onderricht in de Russische taal op de middelbare scholen in te voeren.

XII

De uitspraak van van den Bergh, dat de bemande ruimtevaart onmogelijk, onnodig en misdadig is, steunt op een weinig steekhoudend betoog.

Aarde en wereld in ruimte en tijd, Prof. Mr. Dr. G. van den Bergh, N.V. Em. Querido's Uitgev., Amsterdam, 1960, 347-362.